



New structure-preserving mixed finite element method for the stationary MHD equations with magnetic-current formulation

Xiaodi Zhang^{1,2,3}  · Shitian Dong⁴

Received: 22 May 2023 / Accepted: 4 October 2023 / Published online: 1 November 2023
© The Author(s), under exclusive licence to Springer Nature B.V. 2023

Abstract

In this paper, we propose and analyze a new structure-preserving finite element method for the stationary magnetohydrodynamic equations with magnetic-current formulation on Lipschitz domains. Using a mixed finite element approach, we discretize the hydrodynamic unknowns by inf-sup stable velocity-pressure finite element pairs, and the current density, the induced electric field and the magnetic field by using the edge-edge-face elements from a discrete de-Rham complex pair. To deal with the divergence-free condition of the magnetic field, we introduce an augmented term to the discrete scheme rather than a Lagrange multiplier in the existing schemes. Thanks to discrete differential forms and finite element exterior calculus, the proposed scheme preserves the divergence-free property exactly for the magnetic induction on the discrete level. The well-posedness of the discrete problem is further proved under the small data condition. Under weak regularity assumptions, we rigorously establish the error estimates of the finite element schemes. Numerical results are provided to illustrate the theoretical results and demonstrate the efficiency of the proposed method.

Keywords MHD equations · Finite element method · Divergence-free · Error estimate · de-Rham complex

✉ Xiaodi Zhang
zhangxiaodi@lsec.cc.ac.cn
Shitian Dong
cmd@stu.xju.edu.cn

- ¹ Henan Academy of Big Data, Zhengzhou University, Zhengzhou 450052, China
- ² School of Mathematics and Statistics, Zhengzhou University, Zhengzhou 450001, China
- ³ Key Laboratory of Computing and Stochastic Mathematics (Ministry of Education), School of Mathematics and Statistics, Hunan Normal University, Changsha 410081, Hunan, People's Republic of China
- ⁴ College of Mathematics and System Sciences, Xinjiang University, Urumqi 830046, China

Mathematics Subject Classification 65M12 · 65N30 · 76M10

1 Introduction

Magnetohydrodynamic (MHD) system describes the dynamic behaviors of an electrically conducting fluid under the influence of an external magnetic field. There are many related applications in industrial such as metallurgical engineering, electromagnetic pumping, stirring of liquid metals and controlled thermonuclear fusion [6, 8, 10, 11]. The model often couples the Navier–Stokes equations for hydrodynamics and Maxwell’s equations for electromagnetism via the Lorentz force and Ohm’s law. We refer to [7, 12, 13, 15, 28, 31] and the references therein for the extensive theoretical and numerical studies including the modeling and PDE analysis of the MHD system.

Let Ω be a simply connected bounded domain with Lipschitz-continuous boundary $\Gamma := \partial\Omega$ in \mathbb{R}^d ($d = 2, 3$). In this paper, we consider numerical approximation of the following incompressible MHD equations:

$$\rho \mathbf{u} \cdot \nabla \mathbf{u} - \eta \Delta \mathbf{u} + \nabla p - \mathbf{J} \times \mathbf{B} = \mathbf{f} \quad \text{in } \Omega, \quad (1.1a)$$

$$\nabla \times \mathbf{E} = \mathbf{0}, \quad \mathbf{J} - \nabla \times \mathbf{H} = \mathbf{0} \quad \text{in } \Omega, \quad (1.1b)$$

$$\nabla \cdot \mathbf{u} = 0, \quad \nabla \cdot \mathbf{B} = 0 \quad \text{in } \Omega, \quad (1.1c)$$

where ρ is the density of fluid, \mathbf{u} is the velocity of fluid, p is the pressure, \mathbf{H} is the magnetic field, \mathbf{B} is the magnetic induction, \mathbf{J} is the current density, and \mathbf{E} is the electric field. To close the equations in (1.1), we supply with the following constitutive equation and Ohm’s law

$$\mathbf{B} = \mu \mathbf{H}, \quad \mathbf{J} = \sigma (\mathbf{E} + \mathbf{u} \times \mathbf{B}) \quad \text{in } \Omega. \quad (1.2)$$

The physical parameters are the dynamic viscosity η , the magnetic permeability μ and the electric conductivity σ . In this paper, we consider the following boundary conditions,

$$\mathbf{u} = \mathbf{0}, \quad \mathbf{B} \cdot \mathbf{n} = 0, \quad \mathbf{E} \times \mathbf{n} = \mathbf{0} \quad \text{on } \Gamma, \quad (1.3)$$

where \mathbf{n} is the unit outer normal vector on Γ .

There have been extensive discussions on numerical methods for the incompressible MHD equations [6, 8, 12, 26, 28, 31]. However, due to the nonlinear coupling and rich structures of MHD systems, the numerical simulation still remains a challenging and active research area. Recently, exactly divergence-free discretizations on the magnetic field \mathbf{B} draw more attentions. Physically, the divergence-free condition of \mathbf{B} is a precise physical law in electromagnetics which implies that there is no monopole of magnet. Moreover, it has been shown that the violation of the divergence-free condition on the discrete level will introduce a strong non-physical force and small perturbations to this condition can lead to large errors in numerical simulation, in [4, 5, 30]. Thus, it is vital to preserve this constraint on the discrete level. We also refer to [21] for further arguments for the importance of this divergence-free condition.

In most of the existing methods, the divergence-free constraint condition for \mathbf{B} is relaxed by adding a Lagrange multiplier $r \in H^1$ [7, 26, 28, 32] or grad-div augmented term $-\nabla \nabla \cdot \mathbf{B}$ [12, 13, 33] to numerical formulations. With these treatments, the discrete magnetic induction \mathbf{B}_h is only weakly divergence-free. In, Hiptmair et al. [15] proposed a fully divergence-free method for the unsteady MHD system by introducing a new vector potential formulation, $\mathbf{B} = \nabla \times \mathbf{A}$. In this way, the constraint condition for \mathbf{B} is kept exactly by the definition, $\mathbf{B}_h := \text{curl} \mathbf{A}_h$. Later, this idea is further studied the stationary incompressible MHD equations in [21, 22]. Different from the previous approach, Hu et al. [16] proposed a magnetic-electric based unsteady MHD model where the electric field \mathbf{E} was kept and regarded as an independent variable. By doing so, $\text{div} \mathbf{B}_h = 0$ is ensured exactly and directly by using mixed finite element methods together with techniques from finite element exterior calculus. Indeed, in their discretization, the Gauss's law is automatically satisfied since Faraday's law still holds exactly on the discrete level. Later in, Ma et al. [23] presented the error estimates for the structure-preserving finite element scheme in [16]. In, Qiu et al. [27] revised the structure-preserving finite element method and proved optimal convergence in the energy norm for solutions with low regularity. Motivated by the energy law, Hu et al. [17] extended this idea to the magnetic-current based unsteady MHD model, where the magnetic induction \mathbf{B} and current density \mathbf{J} are taken as electromagnetic variables instead of retaining the electric field \mathbf{E} explicitly as a variable. However, Faraday's law in the stationary case reads $\nabla \times \mathbf{E} = \mathbf{0}$, which is no longer related to the magnetic field. Consequently, such discretizations for the time-dependent systems can not be directly generalized to the steady systems. To address this, Hu et al. [18] treated Gauss's law as an independent equation in the whole system of magnetic-current based formulation and introduced a Lagrange multiplier to appropriately enforce this law on the discrete level. Furthermore, they showed the existence of solutions to the finite element scheme and established the convergence of Picard iterations and finite element scheme under some conditions.

The purpose of this paper is to propose and analyze a new structure-preserving finite element method for the incompressible MHD equations with magnetic-current formulation on Lipschitz domains. Using a mixed finite element approach, inf-sup stable velocity-pressure space pairs are used to approximate the hydrodynamic variables, and the edge-edge-face elements from a discrete de-Rham complex pair are employed to approximate the current density, the induced electric field and the magnetic field. An augmented term is added to the discrete scheme for dealing with the divergence-free condition of the magnetic field. Thanks to discrete differential forms and finite element exterior calculus, the proposed scheme preserves the divergence-free property exactly for the magnetic induction on the discrete without using magnetic Lagrange multipliers. Using the fixed point theorem, the well-posedness of the discrete problem is proved under the small data condition. In terms of the well-designed projection operators, we further rigorously establish the error estimates of the finite element schemes under weak regularity assumptions. Finally, some numerical experiments are presented to verify the theoretical results and the performance of the finite element scheme.

It is remarkable that while the scheme and analysis are somewhat similar to the ones in [18], there are some distinct different points in the following four aspects,

- (i) The schemes are essentially different from in treating with the divergence-free condition of the magnetic field. The paper used the Lagrangian multiplier method to introduce a magnetic Lagrange multiplier, while we employ the augmented method to a magnetic augmented term. Thanks to the structure-preserving properties of the discrete de-Rham complex, the resulting schemes are equivalent and the magnetic Gauss's law is precisely preserved. From this perspective, our scheme is more efficient.
- (ii) The paper only studied the convergence of the Picard iteration by contraction under the small data condition. In this paper, we use the fixed point theorem to give the well-posedness of the discrete problem. The argument is quite different from that therein.
- (iii) In deriving the error estimate, the paper used the routine approach to deal with the reduced form of the finite element scheme, then recover the error estimates for other variables. Since the discrete adjoint operator only defines for finite element functions, some related consistency terms come into the error analysis. This treatment makes the analysis exclude the lowest order Raviart-Thomas element and the singular solution. Herein, we prove the convergence of the original finite element scheme by using the projection method directly. Thanks to the new strategy, our analysis includes the lowest-order Raviart-Thomas element and only needs to assume weak regularity of the solutions. This demonstrates the convergence of the finite element schemes for singular solutions.
- (iv) No numerical results were given therein, but we give some numerical experiments to verify the theoretical results and the performance of the proposed scheme in this paper.

The paper is organized as follows. In Sect. 2, we introduce some notations and present the stability estimate for the MHD equations. In Sect. 3, we propose a new finite element method for the MHD equations. In Sect. 4, the well-posedness of the discrete problem is provided. In Sect. 5, we deduce the error estimates for the proposed scheme. In Sect. 6, we present some numerical experiments to validate the theoretical results. In Sect. 7, we conclude with a few remarks.

2 Preliminaries

We start by introducing some notations and spaces. As usual, the inner product and norm in $L^2(\Omega)$ are denoted by (\cdot, \cdot) and $\|\cdot\|$, respectively. Let $W^{m,p}(\Omega)$ stand for the standard Sobolev spaces equipped with the standard Sobolev norms $\|\cdot\|_{m,p}$. For $p = 2$, we write $H^m(\Omega)$ for $W^{m,2}(\Omega)$ and its corresponding norm is $\|\cdot\|_m$. We will use the following notations for some spaces,

$$\begin{aligned} V &:= H_0^1(\Omega) = \{v \in H^1(\Omega), v|_\Gamma = 0\}, & Q &:= L_0^2(\Omega) = \{q \in L^2(\Omega), (q, 1) = 0\}, \\ W &:= H_0(\operatorname{curl}, \Omega) = \{M \in L^2(\Omega), \nabla \times M \in L^2(\Omega), n \times M|_\Gamma = \mathbf{0}\}, \\ D &:= H_0(\operatorname{div}, \Omega) \\ &= \{C \in L^2(\Omega), \nabla \cdot C \in L^2(\Omega), n \cdot C|_\Gamma = \mathbf{0}\}, & D^0 &:= \{C \in D, \nabla \cdot C = 0\}. \end{aligned}$$

In the following, \mathbf{H}^{-1} is the dual space of $\mathbf{H}_0^1(\Omega)$, the duality pair between them is denoted by $\langle \cdot, \cdot \rangle$, and $\| \cdot \|_{-1}$ is the standard norm in \mathbf{H}^{-1} ,

$$\|f\|_{-1} = \sup_{v \in \mathbf{H}_0^1(\Omega)} \frac{\langle f, v \rangle}{\|\nabla v\|}.$$

Here and what follows, we use C to denote generic positive constants independent of the discretization parameters, which may take different values at different places.

Eliminating \mathbf{E} and \mathbf{H} but keeping \mathbf{J} , we obtain the incompressible MHD equations with magnetic-current formulation,

$$\rho \mathbf{u} \cdot \nabla \mathbf{u} - \eta \Delta \mathbf{u} + \nabla p - \mathbf{J} \times \mathbf{B} = \mathbf{f} \quad \text{in } \Omega, \tag{2.1a}$$

$$\sigma^{-1} \nabla \times \mathbf{J} - \nabla \times (\mathbf{u} \times \mathbf{B}) = \mathbf{0} \quad \text{in } \Omega, \tag{2.1b}$$

$$\mathbf{J} - \mu^{-1} \nabla \times \mathbf{B} = \mathbf{0} \quad \text{in } \Omega, \tag{2.1c}$$

$$\nabla \cdot \mathbf{u} = 0, \quad \nabla \cdot \mathbf{B} = 0 \quad \text{in } \Omega. \tag{2.1d}$$

Let $L, t_0, B_0, u_0 = L/t_0$ be characteristic quantities of length, time, magnetic induction, and fluid velocity, respectively. We introduce the dimensionless variables as follows

$$\begin{aligned} \mathbf{x} &\leftarrow \mathbf{x}/L, \quad \mathbf{u} \leftarrow \mathbf{u}/u_0, \quad p \leftarrow p/(\rho u_0^2), \quad \mathbf{B} \leftarrow \mathbf{B}/B_0, \quad \mathbf{J} \leftarrow \mathbf{J}/(\sigma u_0 B_0), \\ \mathbf{f} &\leftarrow \mathbf{f}t_0/(\rho u_0). \end{aligned}$$

Then, the MHD system (2.1) can be written in a dimensionless form,

$$\mathbf{u} \cdot \nabla \mathbf{u} - R_e^{-1} \Delta \mathbf{u} + \nabla p - S \mathbf{J} \times \mathbf{B} = \mathbf{f} \quad \text{in } \Omega, \tag{2.2a}$$

$$\nabla \times \mathbf{J} - \nabla \times (\mathbf{u} \times \mathbf{B}) = \mathbf{0} \quad \text{in } \Omega, \tag{2.2b}$$

$$\mathbf{J} - R_m^{-1} \nabla \times \mathbf{B} = \mathbf{0} \quad \text{in } \Omega, \tag{2.2c}$$

$$\nabla \cdot \mathbf{u} = 0, \quad \nabla \cdot \mathbf{B} = 0 \quad \text{in } \Omega, \tag{2.2d}$$

where $R_e = \rho L u_0 / \eta$ is the Reynolds number, $R_m = \mu \sigma L u_0$ is the magnetic Reynolds number and $S = \sigma L B_0^2 / (\rho u_0)$ is the coupling number between the fluid and the magnetic field.

To deal with the issue that the curl operator cannot act on the nonlinear coupling term $\mathbf{u} \times \mathbf{B}$ directly on the discrete level, we introduce a new variable, $\boldsymbol{\sigma} = \mathbf{u} \times \mathbf{B}$, as in [17, 18] to accommodate for the evaluation of the discrete curl operator. Physically, $\boldsymbol{\sigma}$ is a part of \mathbf{J} , known as the induced electric field. Thus, the following model is considered,

$$\mathbf{u} \cdot \nabla \mathbf{u} - R_e^{-1} \Delta \mathbf{u} + \nabla p - S \mathbf{J} \times \mathbf{B} = \mathbf{f} \quad \text{in } \Omega, \tag{2.3a}$$

$$\nabla \times \mathbf{J} - \nabla \times \boldsymbol{\sigma} = \mathbf{0} \quad \text{in } \Omega, \tag{2.3b}$$

$$\boldsymbol{\sigma} - \mathbf{u} \times \mathbf{B} = \mathbf{0} \quad \text{in } \Omega, \tag{2.3c}$$

$$\mathbf{J} - R_m^{-1} \nabla \times \mathbf{B} = \mathbf{0} \quad \text{in } \Omega, \quad (2.3d)$$

$$\nabla \cdot \mathbf{u} = 0, \quad \nabla \cdot \mathbf{B} = 0 \quad \text{in } \Omega. \quad (2.3e)$$

According to (1.2) and (1.3), the boundary conditions for this system read

$$\mathbf{u} = \mathbf{0}, \quad \mathbf{B} \cdot \mathbf{n} = 0, \quad \mathbf{J} \times \mathbf{n} = \mathbf{0}, \quad \boldsymbol{\sigma} \times \mathbf{n} = \mathbf{0} \quad \text{on } \Gamma. \quad (2.4)$$

The well-posedness of the continuous formulation has been discussed in [18]. Here, we only give the basic stability estimate for the model (2.3). By taking the inner product of (2.3a) with \mathbf{u} , using $(\mathbf{u} \cdot \nabla \mathbf{u}, \mathbf{u}) = 0$ and (2.3e), we get

$$R_e^{-1} \|\nabla \mathbf{u}\|^2 = S(\mathbf{J} \times \mathbf{B}, \mathbf{u}) + \langle \mathbf{f}, \mathbf{u} \rangle.$$

By taking the inner product of (2.3b) with $S R_m^{-1} \mathbf{B}$, integrating by parts and using (2.3c) and (2.3d), we have

$$S \|\mathbf{J}\|^2 - S(\mathbf{u} \times \mathbf{B}, \mathbf{J}) = 0.$$

Adding both ensuing equations, we obtain the law of energy dissipation that reads

$$R_e^{-1} \|\nabla \mathbf{u}\|^2 + S \|\mathbf{J}\|^2 = \langle \mathbf{f}, \mathbf{u} \rangle. \quad (2.5)$$

Applying the Cauchy–Schwarz inequality and the Young inequality, we estimate the right-hand side of (2.5) as

$$\langle \mathbf{f}, \mathbf{u} \rangle \leq \|\mathbf{f}\|_{-1} \|\nabla \mathbf{u}\| \leq \frac{R_e^{-1}}{2} \|\nabla \mathbf{u}\|^2 + \frac{R_e}{2} \|\mathbf{f}\|_{-1}^2. \quad (2.6)$$

Plugging (2.6) into (2.5), we get

$$\frac{R_e^{-1}}{2} \|\nabla \mathbf{u}\|^2 + S \|\mathbf{J}\|^2 \leq \frac{R_e}{2} \|\mathbf{f}\|_{-1}^2. \quad (2.7)$$

This stability estimate is basic but important in the design and analysis of numerical methods.

3 Finite element approximation

This section is devoted to giving the mixed finite element method for the MHD equations. For the sake of presenting convenience, we focus on the numerical solving of the MHD system in three dimensional case ($d = 3$). The corresponding results in two dimensional case ($d = 2$) are listed in subsequent remarks.

Let \mathcal{T}_h be a quasi-uniform and shape-regular tetrahedral mesh of Ω . As usual, we introduce the local mesh size $h_K = \text{diam}(K)$ and the global mesh size $h :=$

$\max_{K \in \mathcal{T}_h} h_K$. For any integer $k \geq 0$, let $P_k(K)$ be the space of polynomials of degree k on element K and define $\mathbf{P}_k(K) = P_k(K)^3$.

To approximate the velocity and pressure (\mathbf{u}, p) , we use the conforming finite element pair $(\mathbf{V}_h \times Q_h) \subset (\mathbf{V} \times Q)$, which satisfies the discrete inf-sup condition,

$$\inf_{0 \neq q_h \in Q_h} \sup_{\mathbf{0} \neq \mathbf{v}_h \in \mathbf{V}_h} \frac{(q_h, \operatorname{div} \mathbf{v}_h)}{\|\nabla \mathbf{v}_h\| \|q_h\|} \geq \beta_s, \tag{3.1}$$

where β_s is a positive constant independent of mesh size h . To approximate the magnetic field \mathbf{B} , we employ the conforming finite element space $\mathbf{D}_h \subset \mathbf{D}$. To approximate the current density \mathbf{J} and induced electric field $\boldsymbol{\sigma}$, we adopt the conforming finite element space $\mathbf{W}_h \subset \mathbf{W}$. In addition, the electromagnetic pair should meet the following de-Rham sequence,

$$\begin{array}{ccccccc} H_0^1(\Omega) & \xrightarrow{\operatorname{grad}} & \mathbf{W} & \xrightarrow{\operatorname{curl}} & \mathbf{D} & \xrightarrow{\operatorname{div}} & L_0^2(\Omega) \\ \downarrow \Pi_h^{\operatorname{grad}} & & \downarrow \Pi_h^{\operatorname{curl}} & & \downarrow \Pi_h^{\operatorname{div}} & & \downarrow \Pi_h^0, \\ V_h & \xrightarrow{\operatorname{grad}} & \mathbf{W}_h & \xrightarrow{\operatorname{curl}} & \mathbf{D}_h & \xrightarrow{\operatorname{div}} & S_h \end{array} \tag{3.2}$$

where $V_h \subset H_0^1(\Omega)$ and $S_h \subset L_0^2(\Omega)$ are conforming finite element spaces, $\Pi_h^{\operatorname{grad}}$, $\Pi_h^{\operatorname{curl}}$, $\Pi_h^{\operatorname{div}}$ and Π_h^0 are the corresponding standard interpolation operators. We assume that the finite element spaces possess the following approximation properties ulteriorly. There exists an integer $k \geq 1$ such that the following standard approximation properties hold for $k \geq 1$,

$$\inf_{\mathbf{v}_h \in \mathbf{V}_h} (\|\mathbf{u} - \mathbf{v}_h\| + h \|\nabla(\mathbf{u} - \mathbf{v}_h)\|) \leq Ch^{k+1} \|\mathbf{u}\|_{k+1}, \quad \inf_{q_h \in Q_h} \|p - q_h\| \leq Ch^k \|p\|_k, \tag{3.3}$$

$$\inf_{\mathbf{C}_h \in \mathbf{D}_h} (\|\mathbf{B} - \mathbf{C}_h\| + \|\operatorname{div}(\mathbf{B} - \mathbf{C}_h)\|) \leq Ch^k (\|\mathbf{B}\|_k + \|\operatorname{div} \mathbf{B}\|_k), \tag{3.4}$$

$$\inf_{\mathbf{M}_h \in \mathbf{W}_h} (\|\mathbf{J} - \mathbf{M}_h\| + \|\operatorname{curl}(\mathbf{J} - \mathbf{M}_h)\|) \leq Ch^k (\|\mathbf{J}\|_k + \|\operatorname{curl} \mathbf{J}\|_k). \tag{3.5}$$

Many existing pairs of stable finite element pairs can be available in present setting [3, 9, 19].

We also introduce the discrete curl operator on the discrete level. For any $\mathbf{B} \in L^2(\Omega)$, define $\nabla_h \times \mathbf{B} \in \mathbf{W}_h$ as follows,

$$(\nabla_h \times \mathbf{B}, \mathbf{M}_h) = (\mathbf{B}, \nabla \times \mathbf{M}_h), \quad \forall \mathbf{M}_h \in \mathbf{W}_h.$$

For any $\mathbf{J} \in L^2(\Omega)$, we also define $\Pi_W : L^2(\Omega) \rightarrow \mathbf{W}_h$ to be the L^2 -projection such that $\Pi_W \mathbf{J} \in \mathbf{W}_h$ and satisfies

$$(\Pi_W \mathbf{J}, \mathbf{M}_h) = (\mathbf{J}, \mathbf{M}_h), \quad \forall \mathbf{M}_h \in \mathbf{W}_h. \tag{3.6}$$

For convenience, we define the discrete kernel space of the divergence operator on V_h by

$$V_h^0 = \{v_h \in V_h, \quad (\operatorname{div} v_h, q_h) = 0, \quad \forall q_h \in Q_h\}.$$

Similarly, we introduce the exactly solenoidal function space on D_h by

$$D_h^0 = \{C_h \in D_h, \quad \operatorname{div} C_h = 0\}.$$

From [17, 18], we have the following estimates,

$$\|B_h\| \leq \hat{C}_d \|\nabla_h \times B_h\|, \quad \|B_h\|_{0,3} \leq C_d \|\nabla_h \times B_h\|, \quad \forall B_h \in D_h^0. \tag{3.7}$$

The following Poincaré type inequalities are well-known, which will be frequently used in our proof [9],

$$\|v\|_{0,6} \leq C_p \|\nabla v\|, \quad \|v\|_{0,4}^2 \leq \lambda_2 \|\nabla v\|^2, \quad \forall v \in V. \tag{3.8}$$

where the positive constants C_p and λ_2 only depend on Ω . In order to deal with the convection term in (1.1a), we define the following trilinear form

$$\mathcal{O}(u, v, w) = \frac{1}{2} ((u \cdot \nabla v, w) - (u \cdot \nabla w, v)) \quad \forall u, v, w \in V.$$

It is easy to see that the trilinear form $\mathcal{O}(\cdot, \cdot, \cdot)$ is a skew-symmetric with respect to its last two arguments,

$$\mathcal{O}(u, v, w) = -\mathcal{O}(u, w, v), \quad \forall u, v, w \in V, \tag{3.9}$$

and

$$\mathcal{O}(u, v, v) = 0 \quad \forall u, v \in V. \tag{3.10}$$

Now we are ready to present our new finite element discretization for the MHD system (2.3). It reads: find $(u_h, p_h, B_h, J_h, \sigma_h) \in V_h \times Q_h \times D_h \times W_h \times W_h$, such that for any $(v_h, q_h, C_h, \tau_h, M_h) \in V_h \times Q_h \times D_h \times W_h \times W_h$,

$$R_c^{-1} (\nabla u_h, \nabla v_h) + \mathcal{O}(u_h, u_h, v_h) - (p_h, \nabla \cdot v_h) - S(J_h \times B_h, v_h) = \langle f, v_h \rangle, \tag{3.11a}$$

$$(\nabla \cdot u_h, q_h) = 0, \tag{3.11b}$$

$$(\nabla \times J_h, C_h) - (\nabla \times \sigma_h, C_h) + R_m^{-1} (\nabla \cdot B_h, \nabla \cdot C_h) = 0, \tag{3.11c}$$

$$(\boldsymbol{\sigma}_h, \boldsymbol{\tau}_h) - (\mathbf{u}_h \times \mathbf{B}_h, \boldsymbol{\tau}_h) = 0, \tag{3.11d}$$

$$(\mathbf{J}_h, \mathbf{M}_h) - R_m^{-1}(\mathbf{B}_h, \nabla \times \mathbf{M}_h) = 0. \tag{3.11e}$$

Before further discussions, we present some comments on the above scheme. Although the velocity field \mathbf{u}_h is smooth, the $\mathbf{H}(\text{div})$ -conformality of the magnetic field \mathbf{B}_h cannot guarantee $\mathbf{u}_h \times \mathbf{B}_h \in \mathbf{H}(\text{curl}, \Omega)$. Thus, an additional variable $\boldsymbol{\sigma}_h$ is introduced to address this issue in the above scheme. From (3.11d) and (3.11e), we have

$$\boldsymbol{\sigma}_h = \boldsymbol{\Pi}_W(\mathbf{u}_h \times \mathbf{B}_h), \quad \mathbf{J}_h = R_m^{-1} \nabla_h \times \mathbf{B}_h. \tag{3.12}$$

Thus, using the above identities and the definition of the discrete curl operator $\nabla_h \times$, we formally eliminate $\boldsymbol{\sigma}_h$ and \mathbf{J}_h to get a reduced problem with the unknowns $(\mathbf{u}_h, p_h, \mathbf{B}_h) \in \mathbf{V}_h \times Q_h \times \mathbf{D}_h$,

$$R_e^{-1}(\nabla \mathbf{u}_h, \nabla \mathbf{v}_h) + \mathcal{O}(\mathbf{u}_h, \mathbf{u}_h, \mathbf{v}_h) - (p_h, \nabla \cdot \mathbf{v}_h) - SR_m^{-1}(\nabla_h \times \mathbf{B}_h \times \mathbf{B}_h, \mathbf{v}_h) = (\mathbf{f}, \mathbf{v}_h), \tag{3.13a}$$

$$(\nabla \cdot \mathbf{u}_h, q_h) = 0, \tag{3.13b}$$

$$R_m^{-1}(\nabla_h \times \mathbf{B}_h, \nabla_h \times \mathbf{C}_h) + R_m^{-1}(\nabla \cdot \mathbf{B}_h, \nabla \cdot \mathbf{C}_h) - (\mathbf{u}_h \times \mathbf{B}_h, \nabla_h \times \mathbf{C}_h) = 0, \tag{3.13c}$$

for all $(\mathbf{v}_h, q_h, \mathbf{C}_h) \in \mathbf{V}_h \times Q_h \times \mathbf{D}_h$. It is easy to see these two discrete problems (3.11) and (3.13) are equivalent. Namely, we note that if $(\mathbf{u}_h, p_h, \mathbf{B}_h, \mathbf{J}_h, \boldsymbol{\sigma}_h) \in \mathbf{V}_h \times Q_h \times \mathbf{D}_h \times \mathbf{W}_h \times \mathbf{W}_h$ solves the problem (3.11), then $(\mathbf{u}_h, p_h, \mathbf{B}_h) \in \mathbf{V}_h \times Q_h \times \mathbf{D}_h$ solves the problem (3.13) with the same data. Conversely, if $(\mathbf{u}_h, p_h, \mathbf{B}_h) \in \mathbf{V}_h \times Q_h \times \mathbf{D}_h$ is the solution the problem (3.13), we can use (3.12) to reconstruct $(\mathbf{u}_h, p_h, \mathbf{B}_h, \mathbf{J}_h, \boldsymbol{\sigma}_h) \in \mathbf{V}_h \times Q_h \times \mathbf{D}_h \times \mathbf{W}_h \times \mathbf{W}_h$ which solves the problem (3.11) with the same data.

Clearly, formally eliminating $\boldsymbol{\sigma}_h$ and \mathbf{J}_h yields a form that uses only \mathbf{B}_h as the variable of the electromagnetic field. Compared with the \mathbf{B} -based schemes in [12, 13, 27, 28], we find that the reduced system (3.13) takes a similar form formally. Specifically, the magnetic field \mathbf{B} is discretized in \mathbf{H}^1 space with the nodal finite elements in [12, 13] and $\mathbf{H}(\text{curl})$ space with the edge elements in [27, 28]. With these discretizations, the curl operator can act on \mathbf{B} straightway. Different from them, we discretize \mathbf{B} in $\mathbf{H}(\text{div})$ space with the face elements in this paper. Thus, the curl operator $\nabla \times$ can act on \mathbf{B} directly and it is replaced by the discrete curl operator $\nabla_h \times$. This revision leads to a new mixed formulation and makes the analysis essentially different from [12, 13, 27, 28].

What calls for special attention is that the scheme in [18] introduce a Lagrange multiplier to enforce the divergence-free condition of \mathbf{B} , while we deal with this constraint by adding an augmented term $R_m^{-1}(\nabla \cdot \mathbf{B}_h, \nabla \cdot \mathbf{C}_h)$ in the discrete variational formulation. Thanks to the structure-preserving properties of the discrete de-Rham complex, we can design a finite element scheme for stationary MHD problems without using Lagrange multipliers. The resulting scheme is equivalent to the scheme with using the Lagrange multiplier and the magnetic Gauss’s law is precisely preserved.

4 Well-posedness

In this section, we present the well-posedness of the discrete problem. First, we establish some stability estimates for the solution to (3.11), which will be helpful in the subsequent analysis.

Theorem 4.1 *The discrete solution $(\mathbf{u}_h, p_h, \mathbf{B}_h, \mathbf{J}_h, \boldsymbol{\sigma}_h)$ satisfies*

$$R_e^{-1} \|\nabla \mathbf{u}_h\|^2 + S \|\mathbf{J}_h\|^2 = \langle \mathbf{f}, \mathbf{u}_h \rangle. \quad (4.1)$$

Consequently, we have

$$\frac{R_e^{-1}}{2} \|\nabla \mathbf{u}_h\|^2 + S \|\mathbf{J}_h\|^2 \leq \frac{R_e}{2} \|\mathbf{f}\|_{-1}^2. \quad (4.2)$$

In addition, the magnetic field is exactly divergence-free,

$$\nabla \cdot \mathbf{B}_h = 0. \quad (4.3)$$

Proof Taking $(\mathbf{v}_h, q_h, \mathbf{C}_h, \boldsymbol{\tau}_h, \mathbf{M}_h) = (\mathbf{u}_h, p_h, SR_m^{-1} \mathbf{B}_h, S \mathbf{J}_h, S \mathbf{J}_h)$ in (3.11) and adding the five equations together, we obtain

$$R_e^{-1} \|\nabla \mathbf{u}_h\|^2 + S \|\mathbf{J}_h\|^2 + S(\boldsymbol{\sigma}_h, \mathbf{J}_h) - SR_m^{-1}(\nabla \times \boldsymbol{\sigma}_h, \mathbf{B}_h) = \langle \mathbf{f}, \mathbf{u}_h \rangle. \quad (4.4)$$

To deal with the last two terms on the left-hand side of (4.4), we take $\mathbf{M}_h = S \boldsymbol{\sigma}_h$ in (3.11e) to get

$$S(\mathbf{J}_h, \boldsymbol{\sigma}_h) - SR_m^{-1}(\mathbf{B}_h, \nabla \times \boldsymbol{\sigma}_h) = 0. \quad (4.5)$$

Plugging (4.5) into (4.4), we complete the proof of (4.1). For the proof of (4.2), we use the Cauchy–Schwarz inequality and the Young inequality to estimate the right-hand side of (4.4) as

$$\langle \mathbf{f}, \mathbf{u}_h \rangle \leq \|\mathbf{f}\|_{-1} \|\nabla \mathbf{u}_h\| \leq \frac{R_e^{-1}}{2} \|\nabla \mathbf{u}_h\|^2 + \frac{R_e}{2} \|\mathbf{f}\|_{-1}^2. \quad (4.6)$$

Thus, we get (4.2).

For the second part, using the de-Rham sequence (3.2), we obtain $\nabla \times \mathbf{W}_h \subset \mathbf{D}_h$. Taking $\mathbf{C}_h = \nabla \times \mathbf{J}_h - \nabla \times \boldsymbol{\sigma}_h$ in (3.11c) and applying the vector identity, $\nabla \cdot (\nabla \times \mathbf{a}) = 0$, we have

$$\|\nabla \times \mathbf{J}_h - \nabla \times \boldsymbol{\sigma}_h\|^2 = 0,$$

which means that

$$\nabla \times \mathbf{J}_h - \nabla \times \boldsymbol{\sigma}_h = \mathbf{0}. \quad (4.7)$$

Plugging (4.7) into (3.11c), we get

$$R_m^{-1} (\nabla \cdot \mathbf{B}_h, \nabla \cdot \mathbf{C}_h) = 0, \quad \forall \mathbf{C}_h \in \mathbf{D}_h. \tag{4.8}$$

Thus, the estimate (4.3) is deduced by taking $\mathbf{C}_h = \mathbf{B}_h$ in the above equation. \square

Indeed, the current density is weakly divergence-free in the sense that

$$(\mathbf{J}_h, \nabla v_h) = 0 \quad \forall v_h \in V_h,$$

where $V_h \subset H_0^1(\Omega)$ is defined in (3.2). The argument is using the fact $\nabla V_h \subset \mathbf{W}_h$ in (3.2) to take $\mathbf{M}_h = \nabla v_h$ in (3.11e). Furthermore, inspired by the Ohm’s law (1.2), we define the discrete electric field as $\mathbf{E}_h := \mathbf{J}_h - \sigma_h$. Using (4.7), we get the electric field is exactly curl-free, which means that Faraday’s law also holds exactly on the discrete level.

Next, we discuss the well-posedness of the discrete problem (3.11). Here and in what follows, we define the energy norms on the product space $\mathbf{V}_h \times \mathbf{D}_h$ by

$$\|(\mathbf{u}_h, \mathbf{B}_h)\|_1 = \left(R_e^{-1} \|\nabla \mathbf{u}_h\|^2 + SR_m^{-2} \|\nabla_h \times \mathbf{B}_h\|^2 \right)^{1/2}. \tag{4.9}$$

Furthermore, we define the discrete kernel space of $\mathbf{V}_h \times \mathbf{D}_h$, $\mathcal{Y}_h = \mathbf{V}_h^0 \times \mathbf{D}_h^0$. For the sake of convenience, we deal with the well-posedness for the reduced form of the finite element scheme (3.13), then the well-posedness of the primary finite element scheme (3.11) follows by using the equivalence.

Theorem 4.2 For $f \in \mathbf{H}^{-1}(\Omega)$, suppose

$$\mu := \sqrt{2} \max \left\{ \lambda_2 R_e^2, C_p C_d R_e R_m \right\} \|f\|_{-1} < 1, \tag{4.10}$$

then the discrete problem (3.11) is well-posed.

Proof We will first define a mapping $\mathcal{S} : \mathcal{Y}_h \rightarrow \mathcal{Y}_h$, then show that the mapping is a contraction on a subset of \mathcal{Y}_h and apply the Banach fixed point theorem for the existence and uniqueness of the solution. The proof consists of two steps.

Step 1: The mapping \mathcal{S} . We start with defining the mapping \mathcal{S} . Given $(\bar{\mathbf{u}}_h, \bar{\mathbf{B}}_h) \in \mathcal{Y}_h$, we take $\mathcal{S}(\bar{\mathbf{u}}_h, \bar{\mathbf{B}}_h)$ to be the component $(\mathbf{u}_h, \mathbf{B}_h)$ of the solution $(\mathbf{u}_h, p_h, \mathbf{B}_h) \in \mathbf{V}_h \times Q_h \times \mathbf{D}_h$ to the following problem

$$R_e^{-1} (\nabla \mathbf{u}_h, \nabla \mathbf{v}_h) + \mathcal{O}(\bar{\mathbf{u}}_h, \mathbf{u}_h, \mathbf{v}_h) - (p_h, \nabla \cdot \mathbf{v}_h) - SR_m^{-1} (\nabla_h \times \mathbf{B}_h \times \bar{\mathbf{B}}_h, \mathbf{v}_h) = \langle f, \mathbf{v}_h \rangle, \tag{4.11a}$$

$$(\nabla \cdot \mathbf{u}_h, q_h) = 0, \tag{4.11b}$$

$$R_m^{-1} (\nabla_h \times \mathbf{B}_h, \nabla_h \times \mathbf{C}_h) + R_m^{-1} (\nabla \cdot \mathbf{B}_h, \nabla \cdot \mathbf{C}_h) - (\mathbf{u}_h \times \bar{\mathbf{B}}_h, \nabla_h \times \mathbf{C}_h) = 0, \tag{4.11c}$$

for all $(\mathbf{v}_h, q_h, \mathbf{C}_h) \in \mathbf{V}_h \times \mathcal{Q}_h \times \mathbf{D}_h$. From the saddle theory in [9], it is easy to prove that the considered problem (4.11) has a unique solution. In particular, similar to the second part of Theorem 4.1, we deduce that the discrete magnetic field is exactly divergence-free. Using the definition of the discrete curl operator and the fact $\nabla \times \mathbf{W}_h \subset \mathbf{D}_h$, we introduce $\boldsymbol{\sigma}_h := \Pi_W(\mathbf{u}_h \times \bar{\mathbf{B}}_h) \in \mathbf{W}_h$ and $\mathbf{J}_h := R_m^{-1} \nabla_h \times \mathbf{B}_h \in \mathbf{W}_h$ to recast the equation (4.11c) as

$$(\nabla \times \mathbf{J}_h, \mathbf{C}_h) + R_m^{-1} (\nabla \cdot \mathbf{B}_h, \nabla \cdot \mathbf{C}_h) - (\boldsymbol{\sigma}_h, \nabla_h \times \mathbf{C}_h) = 0,$$

for all $\mathbf{C}_h \in \mathbf{D}_h$. Then, similar to the second part of Theorem 4.1, we can easily get $\mathbf{B}_h \in \mathbf{D}_h^0$. Furthermore, setting $(\mathbf{v}_h, q_h, \mathbf{C}_h) = (\mathbf{u}_h, p_h, SR_m^{-1} \mathbf{B}_h)$ and adding the resulting equations together, we have that

$$R_e^{-1} \|\nabla \mathbf{u}_h\|^2 + SR_m^{-2} \|\nabla_h \times \mathbf{B}_h\|^2 = \langle \mathbf{f}, \mathbf{u}_h \rangle. \tag{4.12}$$

Using (4.9), we further get

$$\|(\mathbf{u}_h, \mathbf{B}_h)\|_1^2 \leq \|\mathbf{f}\|_{-1} \|\nabla \mathbf{u}_h\| \leq \sqrt{R_e} \|\mathbf{f}\|_{-1} \|(\mathbf{u}_h, \mathbf{B}_h)\|_1,$$

which yields that

$$\|(\mathbf{u}_h, \mathbf{B}_h)\|_1 \leq \sqrt{R_e} \|\mathbf{f}\|_{-1}. \tag{4.13}$$

Inspired by this, we define a subset of \mathcal{Y}_h by setting

$$B_R = \{(\mathbf{v}_h, \mathbf{C}_h) \in \mathcal{Y}_h : \|(\mathbf{u}_h, \mathbf{B}_h)\|_1 \leq R\},$$

where $R := \sqrt{R_e} \|\mathbf{f}\|_{-1}$. Thus, we consider a map on B_R ,

$$\mathcal{S} : B_R \rightarrow B_R, \quad (\bar{\mathbf{u}}_h, \bar{\mathbf{B}}_h) \mapsto (\mathbf{u}, \mathbf{B}).$$

Obviously, the mapping \mathcal{S} is well defined.

Step 2: The operator \mathcal{S} is a contraction on B_R . To prove this, let $(\bar{\mathbf{u}}_h^i, \bar{\mathbf{B}}_h^i) \in B_R$ and $(\mathbf{u}_h^i, \mathbf{B}_h^i) = \mathcal{S}(\bar{\mathbf{u}}_h^i, \bar{\mathbf{B}}_h^i)$, $i = 1, 2$. By definition, there exist p_h^i such that $(\bar{\mathbf{u}}_h^i, \bar{\mathbf{B}}_h^i)$ and $(\mathbf{u}_h^i, p^i, \mathbf{B}_h^i)$ satisfy

$$R_e^{-1} (\nabla \mathbf{u}_h^i, \nabla \mathbf{v}_h) + \mathcal{O}(\bar{\mathbf{u}}_h^i, \mathbf{u}_h^i, \mathbf{v}_h) - (p_h^i, \nabla \cdot \mathbf{v}_h) - SR_m^{-1} (\nabla_h \times \mathbf{B}_h^i \times \bar{\mathbf{B}}_h^i, \mathbf{v}_h) = \langle \mathbf{f}, \mathbf{v}_h \rangle, \tag{4.14a}$$

$$(\nabla \cdot \mathbf{u}_h^i, q_h) = 0, \tag{4.14b}$$

$$R_m^{-1} (\nabla_h \times \mathbf{B}_h^i, \nabla_h \times \mathbf{C}_h) + R_m^{-1} (\nabla \cdot \mathbf{B}_h^i, \nabla \cdot \mathbf{C}_h) - (\mathbf{u}_h^i \times \bar{\mathbf{B}}_h^i, \nabla_h \times \mathbf{C}_h) = 0, \tag{4.14c}$$

for all $(\mathbf{v}_h, q_h, \mathbf{C}_h) \in \mathbf{V}_h \times Q_h \times \mathbf{D}_h$. We set $\delta_\xi := \xi_h^1 - \xi_h^2$, $\xi = \mathbf{u}, \bar{\mathbf{u}}, p, \mathbf{B}, \bar{\mathbf{B}}$. Subtracting (4.14) as $i = 2$ from (4.14) as $i = 1$, we have

$$R_e^{-1} (\nabla \delta_u, \nabla \mathbf{v}_h) + \mathcal{O}(\bar{\mathbf{u}}_h^1, \mathbf{u}_h^1, \mathbf{v}_h) - \mathcal{O}(\bar{\mathbf{u}}_h^2, \mathbf{u}_h^2, \mathbf{v}_h) - (\delta_p, \nabla \cdot \mathbf{v}_h) - SR_m^{-1} (\nabla_h \times \mathbf{B}_h^1 \times \bar{\mathbf{B}}_h^1, \mathbf{v}_h) + SR_m^{-1} (\nabla_h \times \mathbf{B}_h^2 \times \bar{\mathbf{B}}_h^2, \mathbf{v}_h) = 0, \tag{4.15a}$$

$$(\nabla \cdot \delta_u, q_h) = 0, \tag{4.15b}$$

$$R_m^{-1} (\nabla_h \times \delta_B, \nabla_h \times \mathbf{C}_h) + R_m^{-1} (\nabla \cdot \delta_B, \nabla \cdot \mathbf{C}_h) - (\mathbf{u}_h^1 \times \bar{\mathbf{B}}_h^1, \nabla_h \times \mathbf{C}_h) + (\mathbf{u}_h^2 \times \bar{\mathbf{B}}_h^2, \nabla_h \times \mathbf{C}_h) = 0, \tag{4.15c}$$

for all $(\mathbf{v}_h, q_h, \mathbf{C}_h) \in \mathbf{V}_h \times Q_h \times \mathbf{D}_h$. Taking $(\mathbf{v}_h, q_h, \mathbf{C}_h) = (\delta_u, \delta_p, SR_m^{-1} \delta_B)$, adding the resulting equations together and using the fact that $\mathbf{B}_h^i \in \mathbf{D}_h^0$, $i = 1, 2$, we deduce that

$$R_e^{-1} \|\nabla \delta_u\|^2 + SR_m^{-2} \|\nabla_h \times \delta_B\|^2 = \mathcal{O}(\bar{\mathbf{u}}_h^2, \mathbf{u}_h^2, \delta_u) - \mathcal{O}(\bar{\mathbf{u}}_h^1, \mathbf{u}_h^1, \delta_u) + SR_m^{-1} (\nabla_h \times \mathbf{B}_h^1 \times \bar{\mathbf{B}}_h^1, \delta_u) - SR_m^{-1} (\nabla_h \times \mathbf{B}_h^2 \times \bar{\mathbf{B}}_h^2, \delta_u) + SR_m^{-1} (\mathbf{u}_h^1 \times \bar{\mathbf{B}}_h^1, \nabla_h \times \delta_B) - SR_m^{-1} (\mathbf{u}_h^2 \times \bar{\mathbf{B}}_h^2, \nabla_h \times \delta_B) = I_u + I_B. \tag{4.16}$$

For the term I_u , using Hölder inequality, (3.10) and (3.8), we bound it as follows,

$$I_u = \mathcal{O}(\bar{\mathbf{u}}_h^2, \mathbf{u}_h^2, \delta_u) - \mathcal{O}(\bar{\mathbf{u}}_h^1, \mathbf{u}_h^1, \delta_u) + \mathcal{O}(\bar{\mathbf{u}}_h^1, \mathbf{u}_h^2, \delta_u) - \mathcal{O}(\bar{\mathbf{u}}_h^1, \mathbf{u}_h^1, \delta_u) = -\mathcal{O}(\delta_{\bar{\mathbf{u}}}, \mathbf{u}_h^2, \delta_u) - \mathcal{O}(\bar{\mathbf{u}}_h^1, \delta_u, \delta_u) = -\mathcal{O}(\delta_{\bar{\mathbf{u}}}, \mathbf{u}_h^2, \delta_u) \leq \frac{1}{2} \|\delta_{\bar{\mathbf{u}}}\|_{0,4} \|\nabla \mathbf{u}_h^2\| \|\delta_u\|_{0,4} + \frac{1}{2} \|\delta_{\bar{\mathbf{u}}}\|_{0,4} \|\nabla \delta_u\| \|\mathbf{u}_h^2\|_{0,4} \leq \lambda_2 \|\nabla \mathbf{u}_h^2\| \|\nabla \delta_{\bar{\mathbf{u}}}\| \|\nabla \delta_u\|. \tag{4.17}$$

For the term I_B , we rearrange them as follows:

$$I_B = SR_m^{-1} (\nabla_h \times \mathbf{B}_h^1 \times \bar{\mathbf{B}}_h^1, \delta_u) - SR_m^{-1} (\nabla_h \times \mathbf{B}_h^2 \times \bar{\mathbf{B}}_h^1, \delta_u) + SR_m^{-1} (\nabla_h \times \mathbf{B}_h^2 \times \bar{\mathbf{B}}_h^1, \delta_u) - SR_m^{-1} (\nabla_h \times \mathbf{B}_h^2 \times \bar{\mathbf{B}}_h^2, \delta_u)$$

$$\begin{aligned}
 &+ SR_m^{-1} \left(\mathbf{u}_h^1 \times \bar{\mathbf{B}}_h^1, \nabla_h \times \delta_{\mathbf{B}} \right) - SR_m^{-1} \left(\mathbf{u}_h^2 \times \bar{\mathbf{B}}_h^1, \nabla_h \times \delta_{\mathbf{B}} \right) \\
 &+ SR_m^{-1} \left(\mathbf{u}_h^2 \times \bar{\mathbf{B}}_h^1, \nabla_h \times \delta_{\mathbf{B}} \right) - SR_m^{-1} \left(\mathbf{u}_h^2 \times \bar{\mathbf{B}}_h^2, \nabla_h \times \delta_{\mathbf{B}} \right) \\
 &= SR_m^{-1} \left(\nabla_h \times \delta_{\mathbf{B}} \times \bar{\mathbf{B}}_h^1, \delta_{\mathbf{u}} \right) + SR_m^{-1} \left(\nabla_h \times \mathbf{B}_h^2 \times \delta_{\bar{\mathbf{B}}}, \delta_{\mathbf{u}} \right) \\
 &\quad + SR_m^{-1} \left(\delta_{\mathbf{u}} \times \bar{\mathbf{B}}_h^1, \nabla_h \times \delta_{\mathbf{B}} \right) + SR_m^{-1} \left(\mathbf{u}_h^2 \times \delta_{\bar{\mathbf{B}}}, \nabla_h \times \delta_{\mathbf{B}} \right) \\
 &= SR_m^{-1} \left(\nabla_h \times \mathbf{B}_h^2 \times \delta_{\bar{\mathbf{B}}}, \delta_{\mathbf{u}} \right) + SR_m^{-1} \left(\mathbf{u}_h^2 \times \delta_{\bar{\mathbf{B}}}, \nabla_h \times \delta_{\mathbf{B}} \right),
 \end{aligned}$$

where we have used the fact $(\mathbf{a} \times \mathbf{b}, \mathbf{c}) + (\mathbf{c} \times \mathbf{b}, \mathbf{a}) = 0$ to cancel the first and third terms out in last equality. Using Hölder inequality, (3.7), (3.8) and Young inequality, we get

$$\begin{aligned}
 I_{\mathbf{B}} &\leq SR_m^{-1} \left\| \nabla_h \times \mathbf{B}_h^2 \right\| \left\| \delta_{\bar{\mathbf{B}}} \right\|_{0,3} \left\| \delta_{\mathbf{u}} \right\|_{0,6} \\
 &\quad + SR_m^{-1} \left\| \mathbf{u}_h^2 \right\|_{0,6} \left\| \delta_{\bar{\mathbf{B}}} \right\|_{0,3} \left\| \nabla_h \times \delta_{\mathbf{B}} \right\| \\
 &\leq C_p C_d SR_m^{-1} \left\| \nabla_h \times \mathbf{B}_h^2 \right\| \left\| \nabla_h \times \delta_{\bar{\mathbf{B}}} \right\| \left\| \nabla \delta_{\mathbf{u}} \right\| \\
 &\quad + C_p C_d SR_m^{-1} \left\| \nabla \mathbf{u}_h^2 \right\| \left\| \nabla_h \times \delta_{\bar{\mathbf{B}}} \right\| \left\| \nabla_h \times \delta_{\mathbf{B}} \right\| \\
 &= C_p C_d \sqrt{SR_e} \left\| \nabla_h \times \delta_{\bar{\mathbf{B}}} \right\| \\
 &\quad \left(\sqrt{SR_e^{-1} R_m^{-1}} \left\| \nabla_h \times \mathbf{B}_h^2 \right\| \left\| \nabla \delta_{\mathbf{u}} \right\| + \sqrt{SR_e^{-1} R_m^{-1}} \left\| \nabla \mathbf{u}_h^2 \right\| \left\| \nabla_h \times \delta_{\mathbf{B}} \right\| \right) \\
 &\leq C_p C_d \sqrt{SR_e} \left\| \nabla_h \times \delta_{\bar{\mathbf{B}}} \right\| \left\| (\mathbf{u}_h^2, \mathbf{B}_h^2) \right\|_1 \left\| (\delta_{\mathbf{u}}, \delta_{\mathbf{B}}) \right\|_1. \tag{4.18}
 \end{aligned}$$

Combining (4.17) and (4.18) with (4.16), (4.13) and (4.9), we derive that

$$\begin{aligned}
 \left\| (\delta_{\mathbf{u}}, \delta_{\mathbf{B}}) \right\|_1^2 &\leq \lambda_2 \left\| \nabla \mathbf{u}_h^2 \right\| \left\| \nabla \delta_{\bar{\mathbf{u}}} \right\| \left\| \nabla \delta_{\mathbf{u}} \right\| + C_p C_d \sqrt{SR_e} \left\| \nabla_h \times \delta_{\bar{\mathbf{B}}} \right\| \left\| (\mathbf{u}_h^2, \mathbf{B}_h^2) \right\|_1 \left\| (\delta_{\mathbf{u}}, \delta_{\mathbf{B}}) \right\|_1 \\
 &\leq \max \left\{ \lambda_2 R_e^{\frac{3}{2}}, C_p C_d \sqrt{R_e R_m} \right\} \left\| (\delta_{\bar{\mathbf{u}}}, \delta_{\bar{\mathbf{B}}}) \right\|_1 \\
 &\quad \left(R_e^{-2} \left\| \nabla \mathbf{u}_h^2 \right\|^2 \left\| \nabla \delta_{\mathbf{u}} \right\|^2 + \left\| (\mathbf{u}_h^2, \mathbf{B}_h^2) \right\|_1^2 \left\| (\delta_{\mathbf{u}}, \delta_{\mathbf{B}}) \right\|_1^2 \right)^{\frac{1}{2}} \\
 &\leq \sqrt{2} \max \left\{ \lambda_2 R_e^{\frac{3}{2}}, C_p C_d \sqrt{R_e R_m} \right\} \left\| (\mathbf{u}_h^2, \mathbf{B}_h^2) \right\|_1 \left\| (\delta_{\bar{\mathbf{u}}}, \delta_{\bar{\mathbf{B}}}) \right\|_1 \left\| (\delta_{\mathbf{u}}, \delta_{\mathbf{B}}) \right\|_1 \\
 &\leq \sqrt{2} \max \left\{ \lambda_2 R_e^2, C_p C_d R_e R_m \right\} \left\| f \right\|_{-1} \left\| (\delta_{\bar{\mathbf{u}}}, \delta_{\bar{\mathbf{B}}}) \right\|_1 \left\| (\delta_{\mathbf{u}}, \delta_{\mathbf{B}}) \right\|_1.
 \end{aligned}$$

Thus, we have the estimates for the mapping \mathcal{S} ,

$$\left\| \mathcal{S} \left(\bar{\mathbf{u}}_h^1, \bar{\mathbf{B}}_h^1 \right) - \mathcal{S} \left(\bar{\mathbf{u}}_h^2, \bar{\mathbf{B}}_h^2 \right) \right\|_1 = \left\| (\delta_{\mathbf{u}}, \delta_{\mathbf{B}}) \right\|_1 \leq \mu \left\| (\delta_{\bar{\mathbf{u}}}, \delta_{\bar{\mathbf{B}}}) \right\|_1.$$

By virtue of (4.10), the operator \mathcal{S} is a contraction. As a consequence, an application of the Banach fixed point theorem shows that \mathcal{S} has a fixed point in B_R , which is the solution of problem (3.11). □

Note that we present the existence and uniqueness of the nonlinear scheme (3.13) under the small data condition (4.10) that only contains R_e and R_m , but not S . However, the comparable results obtained in [12, 28, 34] depend on the coupling number. More specifically, S can not be arbitrarily small therein, which seems to be contrary to the physical intuition. The reason why we get such good results is that the energy norm of physical parameter weighting is used (4.10). Under this weighted norm, the paper [18] directly proved the convergence of the Picard iterations by contraction. Although they only studied the convergence of Picard iterations and the argument was quite different from that herein, the small data conditions are almost the same. Following this idea, one can derive similar improved results for the schemes in [12, 28, 34].

5 Error analysis

In this section, we first gather the necessary tools for the error estimates and then carry out a rigorous error analysis for the finite element scheme (3.11). First, we present the classical and discrete Sobolev inequalities needed for the error estimates in the next subsection [9, 18, 27].

Lemma 5.1 For $\mathbf{u} \in \mathbf{H}^{1+s}(\Omega)$ with $s > \frac{1}{2}$, we have

$$\|\mathbf{u}\|_{0,\infty} \leq C_\infty \|\mathbf{u}\|_{1+s}, \quad \|\nabla \mathbf{u}\|_{0,3} \leq C_e \|\mathbf{u}\|_{1+s}.$$

For $\mathbf{J} \in \mathbf{H}^s(\Omega)$ with $s > \frac{1}{2}$, we have

$$\|\mathbf{J}\|_{0,3} \leq C_m \|\mathbf{J}\|_s.$$

Next, we define some projections of the unknowns and gather their approximation properties. For the fluid pair (\mathbf{u}, p) , we define the Stokes projection $(\Pi_V \mathbf{u}, \Pi_Q p) \in \mathbf{V}_h \times Q_h$ such that for all $(\mathbf{v}_h, q_h) \in \mathbf{V}_h \times Q_h$,

$$R_e^{-1}(\nabla \Pi_V \mathbf{u}, \nabla \mathbf{v}_h) - (\Pi_Q p, \nabla \cdot \mathbf{v}_h) = R_e^{-1}(\nabla \mathbf{u}, \nabla \mathbf{v}_h) - (p, \nabla \cdot \mathbf{v}_h), \tag{5.1a}$$

$$(\nabla \cdot \Pi_V \mathbf{u}, q_h) = (\nabla \cdot \mathbf{u}, q_h). \tag{5.1b}$$

For the current density \mathbf{J} and the induced electromotive force $\boldsymbol{\sigma}$, we utilize L^2 -projection defined in (3.6). For the magnetic field \mathbf{B} , notice that $\mathbf{B}_h \in \mathbf{D}_h^0$ and $\mathbf{B} \in \mathbf{D}^0$. We define the L^2 -projection $\Pi_D : L^2(\Omega) \rightarrow \mathbf{D}_h^0$ such that $\Pi_D \mathbf{B} \in \mathbf{D}_h^0$ satisfies,

$$(\Pi_D \mathbf{B}, \mathbf{C}_h) = (\mathbf{B}, \mathbf{C}_h) \quad \forall \mathbf{C}_h \in \mathbf{D}_h^0. \tag{5.2}$$

From [9, 27], we have the following approximation property results for the projections.

Lemma 5.2 Under the regularity assumption (5.5), the above projection satisfies

$$\begin{aligned} \|\nabla(\mathbf{u} - \Pi_V \mathbf{u})\| + \|p - \Pi_Q p\| &\leq Ch^\beta (\|\mathbf{u}\|_{1+\beta} + \|p\|_\beta), \\ \|\mathbf{u} - \Pi_V \mathbf{u}\| &\leq Ch^{\beta+\min\{1,\beta\}} (\|\mathbf{u}\|_{1+\beta} + \|p\|_\beta), \end{aligned}$$

$$\begin{aligned} \|\mathbf{B} - \Pi_D \mathbf{B}\| &\leq Ch^\beta (\|\mathbf{B}\|_\beta + \|\operatorname{div} \mathbf{B}\|_\beta), \\ \|\mathbf{J} - \Pi_D \mathbf{J}\| + \|\operatorname{curl}(\mathbf{J} - \Pi_D \mathbf{J})\| &\leq Ch^\beta (\|\mathbf{J}\|_\beta + \|\operatorname{curl} \mathbf{J}\|_\beta), \\ \|\boldsymbol{\sigma} - \Pi_D \boldsymbol{\sigma}\| + \|\operatorname{curl}(\boldsymbol{\sigma} - \Pi_D \boldsymbol{\sigma})\| &\leq Ch^\beta (\|\boldsymbol{\sigma}\|_\beta + \|\operatorname{curl} \boldsymbol{\sigma}\|_\beta), \end{aligned}$$

with $\beta = \min\{s, k\}$. Moreover, we have

$$\nabla_h \times (\Pi_D \mathbf{B}) = \nabla_h \times \mathbf{B} = \Pi_W (\nabla \times \mathbf{B}). \tag{5.3}$$

Proof Here we only establish the last identity since others have been proved in the references [9, 27]. By using the definitions of $\nabla_h \times$ and Π_D , we can derive that, for any $\mathbf{M}_h \in \mathbf{W}_h$

$$(\nabla_h \times (\Pi_D \mathbf{B}), \mathbf{M}_h) = (\Pi_D \mathbf{B}, \nabla \times \mathbf{M}_h) = (\mathbf{B}, \nabla \times \mathbf{M}_h) = (\nabla_h \times \mathbf{B}, \mathbf{M}_h).$$

Since $\nabla_h \times \mathbf{B}, \nabla_h \times (\Pi_D \mathbf{B}) \in \mathbf{W}_h$, we get $\nabla_h \times (\Pi_D \mathbf{B}) = \nabla_h \times \mathbf{B}$. Similarly, from the definitions of $\nabla_h \times, \Pi_D$ and Π_W , we have for any $\mathbf{M}_h \in \mathbf{W}_h$

$$(\Pi_W (\nabla \times \mathbf{B}), \mathbf{M}_h) = (\nabla \times \mathbf{B}, \mathbf{M}_h) = (\mathbf{B}, \nabla \times \mathbf{M}_h) = (\nabla_h \times \mathbf{B}, \mathbf{M}_h),$$

which finishes the proof by using $\nabla_h \times \mathbf{B}, \Pi_W (\nabla \times \mathbf{B}) \in \mathbf{W}_h$. □

Now we are in the position to derive error estimates for the finite element scheme for the MHD equations. In order to facilitate the subsequent error estimates, we define the following notations here and hereafter

$$e_u = \mathbf{u} - \mathbf{u}_h, \quad e_p = p - p_h, \quad e_B = \mathbf{B} - \mathbf{B}_h, \quad e_J = \mathbf{J} - \mathbf{J}_h, \quad e_\sigma = \boldsymbol{\sigma} - \boldsymbol{\sigma}_h.$$

As usual, the errors are further decomposed into approximation errors and discretization errors

$$e_\zeta = \theta_\zeta + \eta_\zeta, \quad \zeta = \mathbf{u}, p, \mathbf{B}, \mathbf{J}, \boldsymbol{\sigma}. \tag{5.4}$$

The splittings are performed with the previous projections,

$$\begin{aligned} \theta_u &= \mathbf{u} - \Pi_V \mathbf{u}, \\ \theta_p &= p - \Pi_Q p, \quad \theta_B = \mathbf{B} - \Pi_D \mathbf{B}, \quad \theta_J = \mathbf{J} - \Pi_W \mathbf{J}, \\ \theta_\sigma &= \boldsymbol{\sigma} - \Pi_W \boldsymbol{\sigma}, \\ \eta_u &= \Pi_V \mathbf{u} - \mathbf{u}_h, \\ \eta_p &= \Pi_Q p - p_h, \quad \eta_B = \Pi_D \mathbf{B} - \mathbf{B}_h, \\ \eta_J &= \Pi_W \mathbf{J} - \mathbf{J}_h, \quad \eta_\sigma = \Pi_W \boldsymbol{\sigma} - \boldsymbol{\sigma}_h. \end{aligned}$$

By invoking with $\mathbf{J} = R_m^{-1} \nabla \times \mathbf{B}$, (3.12) and (5.3), we have $\eta_J = R_m^{-1} \nabla_h \times \eta_B$.

After the above preparation, we are now in a position to prove the error estimates. For this end, we assume that the exact solution of MHD system (1.1) uniquely exists and the unknowns have the following regularity property:

$$\begin{aligned} \mathbf{u} \in \mathbf{H}^{1+s}(\Omega), \quad p \in H^s(\Omega), \quad \mathbf{B} \in \mathbf{H}^s(\Omega), \quad \mathbf{J}, \nabla \times \mathbf{J} \in \mathbf{H}^s(\Omega), \\ \boldsymbol{\sigma}, \nabla \times \boldsymbol{\sigma} \in \mathbf{H}^s(\Omega), \end{aligned} \tag{5.5}$$

where $s > \frac{1}{2}$. Under this assumption, our main error estimate result can be summarized as follows.

Theorem 5.1 *Let $(\mathbf{u}, p, \mathbf{B}, \mathbf{J})$ and $(\mathbf{u}_h, p_h, \mathbf{B}_h, \mathbf{J}_h)$ be the solution of the continuous problem (2.3) and discrete problem (3.11), respectively. Suppose the regularity assumption (5.5) holds. Then we have the following error estimates*

$$R_e^{-1} \|\nabla \mathbf{u} - \nabla \mathbf{u}_h\| + S \|\mathbf{J} - \mathbf{J}_h\| + \|\mathbf{B} - \mathbf{B}_h\| \leq Ch^\beta, \tag{5.6}$$

$$\|p - p_h\| + \|\boldsymbol{\sigma} - \boldsymbol{\sigma}_h\| \leq Ch^\beta, \tag{5.7}$$

with $\beta = \min\{s, k\}$.

Proof First of all, subtracting the numerical system (3.11) from the above system (2.3) and using the definitions of projections (5.1) and (5.2), we can obtain the following error equations for all $(\mathbf{v}_h, q_h, \mathbf{C}_h, \boldsymbol{\tau}_h, \mathbf{M}_h) \in \mathbf{V}_h \times Q_h \times \mathbf{D}_h \times \mathbf{W}_h \times \mathbf{W}_h$,

$$R_e^{-1}(\nabla \eta_{\mathbf{u}}, \nabla \mathbf{v}_h) - (\eta_p, \nabla \cdot \mathbf{v}_h) = \mathcal{C}(\mathbf{v}_h) + \mathcal{M}_1(\mathbf{v}_h), \tag{5.8a}$$

$$(\nabla \cdot \eta_{\mathbf{u}}^n, q) = 0, \tag{5.8b}$$

$$(\nabla \times \eta_{\mathbf{J}}, \mathbf{C}_h) - (\nabla \times \eta_{\boldsymbol{\sigma}}, \mathbf{C}_h) = \mathcal{M}_2(\mathbf{C}_h), \tag{5.8c}$$

$$(\eta_{\boldsymbol{\sigma}}, \boldsymbol{\tau}_h) = \mathcal{M}_3(\boldsymbol{\tau}_h), \tag{5.8d}$$

$$(\eta_{\mathbf{J}}, \mathbf{M}_h) - R_m^{-1}(\eta_{\mathbf{B}}, \nabla \times \mathbf{M}_h) = \mathcal{M}_4(\mathbf{M}_h), \tag{5.8e}$$

where the abbreviated terms are gathered as

$$\begin{aligned} \mathcal{C}(\mathbf{v}_h) &= \mathcal{O}(\mathbf{u}_h, \mathbf{u}_h, \mathbf{v}_h) - \mathcal{O}(\mathbf{u}, \mathbf{u}, \mathbf{v}_h), \\ \mathcal{M}_1(\mathbf{v}_h) &= S(\mathbf{J} \times \mathbf{B}, \mathbf{v}_h) - S(\mathbf{J}_h \times \mathbf{B}_h, \mathbf{v}_h), \\ \mathcal{M}_2(\mathbf{C}_h) &= -(\nabla \times \theta_{\mathbf{J}}, \mathbf{C}_h) - (\nabla \times \theta_{\boldsymbol{\sigma}}, \mathbf{C}_h), \\ \mathcal{M}_3(\boldsymbol{\tau}_h) &= (\mathbf{u} \times \mathbf{B}, \boldsymbol{\tau}_h) - (\mathbf{u}_h \times \mathbf{B}_h, \boldsymbol{\tau}_h), \\ \mathcal{M}_4(\mathbf{M}_h) &= R_m^{-1}(\theta_{\mathbf{B}}, \nabla \times \mathbf{M}_h). \end{aligned}$$

Taking $(\mathbf{v}_h, q_h, \mathbf{C}_h, \boldsymbol{\tau}_h, \mathbf{M}_h) = (\eta_{\mathbf{u}}, \eta_p, SR_m^{-1}\eta_{\mathbf{B}}, S\eta_{\mathbf{J}}, S\eta_{\mathbf{J}})$ in (5.8) and adding the five equations together, we obtain

$$\begin{aligned} R_e^{-1} \|\nabla \eta_{\mathbf{u}}\|^2 + S \|\eta_{\mathbf{J}}\|^2 + S(\eta_{\boldsymbol{\sigma}}, \eta_{\mathbf{J}}) - SR_m^{-1}(\nabla \times \eta_{\boldsymbol{\sigma}}, \eta_{\mathbf{B}}) \\ = \mathcal{C}(\eta_{\mathbf{u}}) + \mathcal{M}_1(\eta_{\mathbf{u}}) + S\mathcal{M}_3(\eta_{\mathbf{J}}) + SR_m^{-1}\mathcal{M}_2(\eta_{\mathbf{B}}) + S\mathcal{M}_4(\eta_{\mathbf{J}}). \end{aligned} \tag{5.9}$$

To deal with the last two terms on the left-hand side of (5.9), we take $\mathbf{M}_h = S\eta_\sigma$ in (5.8e) to get

$$S(\eta_J, \eta_\sigma) - SR_m^{-1}(\eta_B, \nabla \times \eta_\sigma) = S\mathcal{M}_4(\eta_\sigma). \tag{5.10}$$

Plugging (5.10) into (5.9) yields

$$\begin{aligned} & R_\epsilon^{-1} \|\nabla \eta_u\|^2 + S \|\eta_J\|^2 \\ &= \mathcal{C}(\eta_u) + \mathcal{M}_1(\eta_u) + S\mathcal{M}_3(\eta_J) + SR_m^{-1} \mathcal{M}_2(\eta_B) \\ & \quad + S\mathcal{M}_4(\eta_J) - S\mathcal{M}_4(\eta_\sigma). \end{aligned} \tag{5.11}$$

We next bound the terms on the right-hand side of the above identity one by one. For the first term on the right-hand side of (5.11), we bound it as follows,

$$\begin{aligned} \mathcal{C}(\eta_u) &= \mathcal{O}(\mathbf{u}_h, \mathbf{u}_h, \eta_u) - \mathcal{O}(\mathbf{u}_h, \mathbf{u}, \eta_u) + \mathcal{O}(\mathbf{u}_h, \mathbf{u}, \eta_u) - \mathcal{O}(\mathbf{u}, \mathbf{u}, \eta_u) \\ &= -\mathcal{O}(\mathbf{e}_u, \mathbf{u}, \eta_u) - \mathcal{O}(\mathbf{u}_h, \mathbf{e}_u, \eta_u) \\ &= -\mathcal{O}(\theta_u, \mathbf{u}, \eta_u) - \mathcal{O}(\eta_u, \mathbf{u}, \eta_u) - \mathcal{O}(\mathbf{u}_h, \theta_u, \eta_u). \end{aligned}$$

The terms in the last step can be bounded using Hölder inequality, ϵ -Young inequality, (2.7), (4.2), Sobolev inequalities in Lemma 5.1 and the approximation properties of the projections in Lemma 5.2 as,

$$\begin{aligned} \mathcal{C}(\eta_u) &\leq \frac{1}{2} \|\theta_u\|_{0,4} \|\nabla \mathbf{u}\| \|\eta_u\|_{0,4} + \frac{1}{2} \|\theta_u\|_{0,4} \|\nabla \eta_u\| \|\mathbf{u}\|_{0,4} \\ & \quad + \frac{1}{2} \|\eta_u\|_{0,4} \|\nabla \mathbf{u}\| \|\eta_u\|_{0,4} + \frac{1}{2} \|\eta_u\|_{0,4} \|\nabla \eta_u\| \|\mathbf{u}\|_{0,4} \\ & \quad + \frac{1}{2} \|\mathbf{u}_h\|_{0,4} \|\nabla \theta_u\| \|\eta_u\|_{0,4} + \frac{1}{2} \|\mathbf{u}_h\|_{0,4} \|\nabla \eta_u\| \|\theta_u\|_{0,4} \\ &\leq \lambda_2 \|\nabla \theta_u\| \|\nabla \mathbf{u}\| \|\nabla \eta_u\| + \lambda_2 \|\nabla \mathbf{u}\| \|\nabla \eta_u\|^2 \\ & \quad + \lambda_2 \|\nabla \mathbf{u}_h\| \|\nabla \theta_u\| \|\nabla \eta_u\| \\ &\leq \left(\lambda_2 \|\nabla \mathbf{u}\| + \epsilon R_\epsilon^{-1} \right) \|\nabla \eta_u\|^2 + C\epsilon^{-1} \|\nabla \theta_u\|^2 \\ &\leq \left(\lambda_2 \|\nabla \mathbf{u}\| + \epsilon R_\epsilon^{-1} \right) \|\nabla \eta_u\|^2 + C\epsilon^{-1} h^{2\beta}, \end{aligned}$$

where the parameter $\epsilon > 0$ will be specified later.

For the second and third terms on the right-hand side of (5.11), we rearrange them as follows:

$$\begin{aligned} \mathcal{M}_1(\eta_u) + S\mathcal{M}_3(\eta_J) &= S((\mathbf{J} - \mathbf{J}_h) \times \mathbf{B}_h, \eta_u) + S(\mathbf{J} \times (\mathbf{B} - \mathbf{B}_h), \eta_u) \\ & \quad + S((\mathbf{u} - \mathbf{u}_h) \times \mathbf{B}_h, \eta_J) + S(\mathbf{u} \times (\mathbf{B} - \mathbf{B}_h), \eta_J) \\ &= M_1 + M_2 + M_3 + M_4. \end{aligned}$$

Next we will estimate $M_1 + M_3$ and $M_2 + M_4$ separately. For the terms $M_1 + M_3$, we have

$$\begin{aligned} M_1 + M_3 &= S((\theta_J + \eta_J) \times \mathbf{B}_h, \eta_u) + S((\theta_u + \eta_u) \times \mathbf{B}_h, \eta_J) \\ &= S(\theta_J \times \mathbf{B}_h, \eta_u) + S(\theta_u \times \mathbf{B}_h, \eta_J) + S(\eta_J \times \mathbf{B}_h, \eta_u) + S(\eta_u \times \mathbf{B}_h, \eta_J) \\ &= S(\theta_J \times \mathbf{B}_h, \eta_u) + S(\theta_u \times \mathbf{B}_h, \eta_J), \end{aligned}$$

where we have used the fact $(\mathbf{a} \times \mathbf{b}, \mathbf{c}) + (\mathbf{c} \times \mathbf{b}, \mathbf{a}) = 0$ to cancel the last two terms out in the last equality. Using Hölder inequality, Young inequality, (3.8), (3.12), (3.7) and (4.2), we get

$$\begin{aligned} M_1 + M_3 &= S(\theta_J \times \mathbf{B}_h, \eta_u) + S(\theta_u \times \mathbf{B}_h, \eta_J) \\ &\leq S \|\theta_J\| \|\mathbf{B}_h\|_{0,3} \|\eta_u\|_{0,6} + S \|\theta_u\|_{0,6} \|\mathbf{B}_h\|_{0,3} \|\eta_J\| \\ &\leq C_p S C_d \|\theta_J\| \|\nabla_h \times \mathbf{B}_h\| \|\nabla \eta_u\| + C_p S C_d \|\nabla \theta_u\| \|\nabla_h \times \mathbf{B}_h\| \|\eta_J\| \\ &\leq C_p S R_m C_d \|\theta_J\| \|\mathbf{J}_h\| \|\nabla \eta_u\| + C_p S R_m C_d \|\nabla \theta_u\| \|\mathbf{J}_h\| \|\eta_J\| \\ &\leq \frac{\epsilon R_e^{-1}}{2} \|\nabla \eta_u\|^2 + \frac{\epsilon S}{2} \|\eta_J\|^2 + C \epsilon^{-1} \|\theta_J\|^2 + C \epsilon^{-1} \|\nabla \theta_u\|^2 \\ &\leq \frac{\epsilon R_e^{-1}}{2} \|\nabla \eta_u\|^2 + \frac{\epsilon S}{2} \|\eta_J\|^2 + C \epsilon^{-1} h^{2\beta}. \end{aligned}$$

For the terms $M_2 + M_4$, we have

$$\begin{aligned} M_2 + M_4 &= S(\mathbf{J} \times (\mathbf{B} - \mathbf{B}_h), \eta_u) + S(\mathbf{u} \times (\mathbf{B} - \mathbf{B}_h), \eta_J) \\ &= S(\mathbf{J} \times \theta_B, \eta_u) + S(\mathbf{u} \times \theta_B, \eta_J) \\ &\quad + S(\mathbf{J} \times \eta_B, \eta_u) + S(\mathbf{u} \times \eta_B, \eta_J). \end{aligned}$$

Applying Hölder inequality, Young inequality, (3.8), Lemma 5.1 and Lemma 5.2, we have

$$\begin{aligned} M_2 + M_4 &\leq S \|\mathbf{J}\|_{0,3} \|\theta_B\| \|\eta_u\|_{0,6} + S \|\mathbf{J}\| \|\eta_B\|_{0,3} \|\eta_u\|_{0,6} \\ &\quad + S \|\mathbf{u}\|_{0,\infty} \|\theta_B\| \|\eta_J\| + S \|\mathbf{u}\|_{0,6} \|\eta_B\|_{0,3} \|\eta_J\| \\ &\leq C_m C_p S \|\mathbf{J}\|_s \|\theta_B\| \|\nabla \eta_u\| + C_p S C_d \|\mathbf{J}\| \|\nabla_h \times \eta_B\| \|\nabla \eta_u\| \\ &\quad + C_\infty S \|\mathbf{u}\|_{1+s} \|\theta_B\| \|\eta_J\| + C_p S C_d \|\nabla \mathbf{u}\| \|\nabla_h \times \eta_B\| \|\eta_J\| \\ &\leq C_m C_p S \|\mathbf{J}\|_s \|\theta_B\| \|\nabla \eta_u\| + C_p S C_d R_m \|\mathbf{J}\| \|\eta_J\| \|\nabla \eta_u\| \\ &\quad + C_\infty S \|\mathbf{u}\|_{1+s} \|\theta_B\| \|\eta_J\| + C_p S C_d R_m \|\nabla \mathbf{u}\| \|\eta_J\|^2 \\ &\leq \frac{\epsilon R_e^{-1}}{2} \|\nabla \eta_u\|^2 + \frac{\epsilon S}{2} \|\eta_J\|^2 + C_p S C_d R_m \|\mathbf{J}\| \|\eta_J\| \|\nabla \eta_u\| \\ &\quad + C_p S C_d R_m \|\nabla \mathbf{u}\| \|\eta_J\|^2 + C \epsilon^{-1} \|\theta_B\|^2 \\ &\leq \frac{\epsilon R_e^{-1}}{2} \|\nabla \eta_u\|^2 + \frac{\epsilon S}{2} \|\eta_J\|^2 + C_p S C_d R_m \|\nabla \mathbf{u}\| \|\eta_J\|^2 \\ &\quad + \frac{C_p C_d R_m \sqrt{S R_e}}{2} \|\mathbf{J}\| \left(R_e^{-1} \|\nabla \eta_u\|^2 + S \|\eta_J\|^2 \right) + C \epsilon^{-1} h^{2\beta}. \end{aligned}$$

Hence, we derive that

$$\begin{aligned} \mathcal{M}_1(\eta_u) + S\mathcal{M}_3(\eta_J) &\leq \epsilon R_e^{-1} \|\nabla \eta_u\|^2 + \epsilon S \|\eta_J\|^2 + C_p S C_d R_m \|\nabla \mathbf{u}\| \|\eta_J\|^2 \\ &\quad + \frac{C_p C_d R_m \sqrt{S R_e}}{2} \|\mathbf{J}\| \left(R_e^{-1} \|\nabla \eta_u\|^2 + S \|\eta_J\|^2 \right) \\ &\quad + C \epsilon^{-1} h^{2\beta}. \end{aligned}$$

For the fourth term on the right-hand side of (5.11), we use the Cauchy-Schwarz inequality, Young inequality and Lemma 5.2 to estimate it as

$$\begin{aligned} S R_m^{-1} \mathcal{M}_2(\eta_B) &= -S R_m^{-1} (\nabla \times \theta_J, \eta_B) - S R_m^{-1} (\nabla \times \theta_\sigma, \eta_B) \\ &\leq S R_m^{-1} \|\nabla \times \theta_J\| \|\eta_B\| + S R_m^{-1} \|\nabla \times \theta_\sigma\| \|\eta_B\| \\ &\leq S R_m^{-1} \hat{C}_d \|\nabla \times \theta_J\| \|\nabla_h \times \eta_B\| + S R_m^{-1} \hat{C}_d \|\nabla \times \theta_\sigma\| \|\nabla_h \times \eta_B\| \\ &= S \hat{C}_d \|\nabla \times \theta_J\| \|\eta_J\| + S \hat{C}_d \|\nabla \times \theta_\sigma\| \|\eta_J\| \\ &\leq \epsilon S \|\eta_J\|^2 + C \epsilon^{-1} \|\nabla \times \theta_J\|^2 + C \epsilon^{-1} \|\nabla \times \theta_\sigma\|^2 \\ &\leq \epsilon S \|\eta_J\|^2 + C \epsilon^{-1} h^{2\beta}. \end{aligned}$$

For the last two terms on the right-hand side of (5.11), we invoke with the fact that $\nabla_h \times \theta_B = \mathbf{0}$ to get

$$\begin{aligned} S\mathcal{M}_4(\eta_J) - S\mathcal{M}_4(\eta_\sigma) &= S R_m^{-1} (\theta_B, \nabla \times (\eta_J - \eta_\sigma)) \\ &= S R_m^{-1} (\nabla_h \times \theta_B, \eta_J - \eta_\sigma) = 0. \end{aligned}$$

Combining all the above and using the Cauchy-Schwarz inequality, we arrive at

$$\begin{aligned} &R_e^{-1} \|\nabla \eta_u^n\|^2 + S \|\eta_J^n\|^2 \\ &\leq \left(\lambda_2 \|\nabla \mathbf{u}\| + 2\epsilon R_e^{-1} \right) \|\nabla \eta_u\|^2 + 2\epsilon S \|\eta_J\|^2 + C_p S C_d R_m \|\nabla \mathbf{u}\| \|\eta_J\|^2 \\ &\quad + \frac{C_p C_d R_m \sqrt{S R_e}}{2} \|\mathbf{J}\| \left(R_e^{-1} \|\nabla \eta_u\|^2 + S \|\eta_J\|^2 \right) + C \epsilon^{-1} h^{2\beta} \\ &\leq \left(\max \{ \lambda_2 R_e, C_p C_d R_m \} \|\nabla \mathbf{u}\| + 2\epsilon \right) \left(R_e^{-1} \|\nabla \eta_u\|^2 + S \|\eta_J\|^2 \right) \\ &\quad + \frac{C_p C_d R_m \sqrt{S R_e}}{2} \|\mathbf{J}\| \left(R_e^{-1} \|\nabla \eta_u\|^2 + S \|\eta_J\|^2 \right) + C \epsilon^{-1} h^{2\beta}, \end{aligned}$$

for any $\epsilon > 0$. Using (4.10) and (4.12), for ϵ being small enough, we derive

$$R_e^{-1} \|\nabla \eta_u^n\|^2 + S \|\eta_J^n\|^2 \leq C h^{2\beta}. \tag{5.12}$$

We complete the proof of \mathbf{H}^1 -norm estimate for the velocity and \mathbf{L}^2 -norm estimate for the current density in (5.6) by applying the triangle inequality, the approximation properties of the projections Lemma 5.2 together with the above estimates.

Then, we give the proof of L^2 -norm estimate for the magnetic field in (5.6). Using (3.7), we have

$$\|\eta_B\| \leq \hat{C}_d \|\nabla_h \times \eta_B\| \leq Ch^{2\beta}. \tag{5.13}$$

Thus, the desired estimate follows the triangle inequality, (5.13) and the approximation properties of the projections Lemma 5.2.

Next, we turn to deduce the L^2 -norm estimate for the induced electric field in (5.7). With the above estimates for u , B and J , we take $\tau_h = \eta_\sigma$ in (5.8d) to get the following equation for σ ,

$$\begin{aligned} \|\eta_\sigma\|^2 &= (u \times e_B, \eta_\sigma) + (e_u \times B_h, \eta_\sigma) \\ &\leq \|u\|_{0,\infty} \|e_B\| \|\eta_\sigma\| + \|e_u\|_{0,6} \|B_h\|_{0,3} \|\eta_\sigma\| \\ &\leq C_\infty \|u\|_{1+s} \|e_B\| \|\eta_\sigma\| + C_p C_d \|\nabla e_u\| \|\nabla_h \times B_h\| \|\eta_\sigma\| \\ &\leq C_\infty \|u\|_{1+s} \|e_B\| \|\eta_\sigma\| + C_p C_d R_m \|\nabla e_u\| \|J_h\| \|\eta_\sigma\|. \end{aligned}$$

Here in the last inequality, we invoke with the Hölder inequality, Sobolev inequality in Lemma 5.1, (3.7) and (3.12). Thus, using the stability of the solution and the error estimates for the velocity and magnetic field (5.13), we have

$$\|\eta_\sigma\| \leq C \|e_B\| + C \|\nabla e_u\|.$$

This completes the proof for the L^2 -norm estimate for the induced electric field in (5.7) with a simple triangle inequality and the approximation properties of the projections Lemma 5.2.

Finally, we give the error estimate for the pressure. From the error equation (5.8a), we have

$$(\eta_p, \nabla \cdot v_h) = R_e^{-1}(\nabla \eta_u, \nabla v_h) - \mathcal{C}(v_h) - \mathcal{M}_1(v_h).$$

Using Cauchy-Schwarz inequality, Hölder inequality, Lemma 5.1, (3.7), (3.12) and (4.2), we obtain

$$\begin{aligned} (\eta_p, \nabla \cdot v_h) &\leq R_e^{-1} \|\nabla \eta_u\| \|\nabla v_h\| + \lambda_2 \|\nabla e_u\| \|\nabla u\| \|\nabla v_h\| \\ &\quad + \lambda_2 \|\nabla u_h\| \|\nabla e_u\| \|\nabla v_h\| + S \|e_J\| \|B_h\|_{0,3} \|v_h\|_{0,6} \\ &\quad + S \|J\|_{0,3} \|e_B\| \|v_h\|_{0,6} \\ &\leq R_e^{-1} \|\nabla \eta_u\| \|\nabla v_h\| + \lambda_2 \|\nabla e_u\| \|\nabla u\| \|\nabla v_h\| \\ &\quad + \lambda_2 \|\nabla u_h\| \|\nabla e_u\| \|\nabla v_h\| + SR_m C_d \|e_J\| \|J_h\| \|v_h\|_{0,6} \\ &\quad + SC_m \|J\|_s \|e_B\| \|v_h\|_{0,6} \\ &\leq C (\|\nabla e_u\| + \|e_J\| + \|e_B\|) \|\nabla v_h\|. \end{aligned}$$

Invoking with the inf-sup condition (3.1), the triangle inequality, the approximation properties of the projections Lemma 5.2, and the error estimates for the velocity,

current density and magnetic field in (5.13), we get

$$\|p - p_h\| \leq \|\eta_p\| + \|\theta_p\| \leq C (\|\nabla e_u\| + \|e_J\| + \|e_B\| + \|\theta_p\|) \leq Ch^\beta,$$

which gives the estimate for the pressure in (5.7). Thus, the proof is complete. \square

Remark 5.1 As a result, from (2.3d), (3.12) and (5.6), it can be inferred that

$$R_m^{-1} \|\nabla \times \mathbf{B} - \nabla_h \times \mathbf{B}_h\| = \|e_J\| \leq Ch^\beta.$$

Remark 5.2 In this paper, we prove the convergence of the original finite element scheme by using the projection method directly. Thanks to the new strategy, our analysis includes the lowest-order Raviart-Thomas element and only needs to assume weak regularity of the solutions. This demonstrates the convergence of the finite element schemes for singular solutions. While the paper [18] used the routine approach to deal with the reduced form of the finite element scheme, then recovered the error estimates for other variables. Since the discrete adjoint operator only is defined for finite element functions, some related consistency terms come into the error analysis. This treatment makes the analysis exclude the lowest-order Raviart-Thomas element and the singular solution.

Remark 5.3 The scheme and results are still applicable to the two dimensional case ($d = 2$). Specifically, when $d = 2$, the induced electric field σ and the current density J are scalar fields in 2D. To replace the space \mathbf{W} in 3D, we define $W := H_0^1(\Omega)$ which can be identified with the scalar valued space $H_0(\mathbf{curl})$. Similarly, the finite element space pair (W_h, \mathbf{D}_h) are chosen from the de-Rham complex in 2D,

$$\begin{array}{ccccc} W & \xrightarrow{\text{curl}} & \mathbf{D} & \xrightarrow{\text{div}} & L_0^2(\Omega) \\ \downarrow \Pi_h^{\text{curl}} & & \downarrow \Pi_h^{\text{div}} & & \downarrow \Pi_h^0 \\ W_h & \xrightarrow{\text{curl}} & \mathbf{D}_h & \xrightarrow{\text{div}} & S_h \end{array} \quad (5.14)$$

In this paper, we employ the linear Lagrange finite element space to define W_h . With these minor modifications, it is easy to see that the presentation in this section is applicable to 2D.

6 Numerical experiments

In this section, we present a series of numerical examples to verify the theoretical results of the proposed schemes. The first example is to verify the rates of convergence for our scheme. The second example is to verify the rates of convergence for the Hartmann flow. The third example is to illustrate the performance by computing the benchmark problem—the lid-driven cavity flow. The finite element method is implemented on the finite element software FreeFEM developed by Hecht et al. [14].

To solve the discrete system (3.11), we employ the fixed point iterative algorithm for solving such a nonlinear system, see (4.11). It can be described as follows,

Fixed point iteration

For given $(\mathbf{u}_h^{n-1}, \mathbf{B}_h^{n-1}) \in V_h^0 \times D_h^0$, find $(\mathbf{u}_h^n, p_h^n, \mathbf{B}_h^n, \mathbf{J}_h^n, \boldsymbol{\sigma}_h^n) \in V_h \times Q_h \times D_h \times \mathbf{W}_h \times \mathbf{W}_h$ such that for all $(\mathbf{v}_h, q_h, \mathbf{C}_h, \boldsymbol{\tau}_h, \mathbf{M}_h) \in V_h \times Q_h \times D_h \times \mathbf{W}_h \times \mathbf{W}_h$,

$$R_e^{-1} (\nabla \mathbf{u}_h^n, \nabla \mathbf{v}_h) + \mathcal{O} (\mathbf{u}_h^{n-1}, \mathbf{u}_h^n, \mathbf{v}_h) - (p_h^n, \nabla \cdot \mathbf{v}_h) - S (\mathbf{J}_h^n \times \mathbf{B}_h^{n-1}, \mathbf{v}_h) = \langle \mathbf{f}, \mathbf{v}_h \rangle, \tag{6.1a}$$

$$(\nabla \cdot \mathbf{u}_h^n, q_h) = 0, \tag{6.1b}$$

$$(\nabla \times \mathbf{J}_h^n, \mathbf{C}_h) - (\nabla \times \boldsymbol{\sigma}_h^n, \mathbf{C}_h) + R_m^{-1} (\nabla \cdot \mathbf{B}_h^n, \nabla \cdot \mathbf{C}_h) = 0, \tag{6.1c}$$

$$(\boldsymbol{\sigma}_h^n, \boldsymbol{\tau}_h) - (\mathbf{u}_h^n \times \mathbf{B}_h^{n-1}, \boldsymbol{\tau}_h) = 0, \tag{6.1d}$$

$$(\mathbf{J}_h^n, \mathbf{M}_h) - R_m^{-1} (\mathbf{B}_h^n, \nabla \times \mathbf{M}_h) = 0, \tag{6.1e}$$

for $n = 1, 2, \dots$, until $\|\mathbf{u}_h^n - \mathbf{u}_h^{n-1}\| + \|\mathbf{B}_h^n - \mathbf{B}_h^{n-1}\| \leq \epsilon_0$. Here, the initial value $(\mathbf{u}_h^0, \mathbf{B}_h^0) \in V_h^0 \times D_h^0$ is defined by

$$R_e^{-1} (\nabla \mathbf{u}_h^0, \nabla \mathbf{v}_h) - (p_h^0, \nabla \cdot \mathbf{v}_h) = \langle \mathbf{f}, \mathbf{v}_h \rangle, \tag{6.2a}$$

$$(\nabla \cdot \mathbf{u}_h^0, q_h) = 0, \tag{6.2b}$$

$$(\nabla \times \mathbf{J}_h^0, \mathbf{C}_h) + R_m^{-1} (\nabla \cdot \mathbf{B}_h^0, \nabla \cdot \mathbf{C}_h) = 0, \tag{6.2c}$$

$$(\mathbf{J}_h^0, \mathbf{M}_h) - R_m^{-1} (\mathbf{B}_h^0, \nabla \times \mathbf{M}_h) = 0, \tag{6.2d}$$

for all $(\mathbf{v}_h, q_h, \mathbf{C}_h, \mathbf{M}_h) \in V_h \times Q_h \times D_h \times \mathbf{W}_h$.

The iterative tolerance $\epsilon_0 = 10^{-6}$ is used in all examples.

For comparison, we also consider the finite element scheme given in [18]. Recall that S_h is the finite element introduced in (3.2), then we have the following inf-sup condition holds,

$$\inf_{0 \neq s_h \in S_h} \sup_{0 \neq \mathbf{C}_h \in D_h} \frac{(s_h, \text{div} \mathbf{C}_h)}{\|\mathbf{C}_h\|_{\text{div}} \|s_h\|} \geq \beta_m, \tag{6.3}$$

where β_m is a positive constant independent of mesh size h . Hence, the finite element scheme with the Lagrange multiplier reads as follows: find $(\mathbf{u}_h, p_h, \mathbf{B}_h, \mathbf{J}_h, \boldsymbol{\sigma}_h, r_h) \in V_h \times Q_h \times D_h \times \mathbf{W}_h \times \mathbf{W}_h \times S_h$, such that for any $(\mathbf{v}_h, q_h, \mathbf{C}_h, \boldsymbol{\tau}_h, \mathbf{M}_h, s_h) \in V_h \times Q_h \times D_h \times \mathbf{W}_h \times \mathbf{W}_h \times S_h$,

$$R_e^{-1} (\nabla \mathbf{u}_h, \nabla \mathbf{v}_h) + \mathcal{O} (\mathbf{u}_h, \mathbf{u}_h, \mathbf{v}_h) - (p_h, \nabla \cdot \mathbf{v}_h) - S (\mathbf{J}_h \times \mathbf{B}_h, \mathbf{v}_h) = \langle \mathbf{f}, \mathbf{v}_h \rangle, \tag{6.4a}$$

$$(\nabla \cdot \mathbf{u}_h, q_h) = 0, \tag{6.4b}$$

$$(\nabla \times \mathbf{J}_h, \mathbf{C}_h) - (\nabla \times \boldsymbol{\sigma}_h, \mathbf{C}_h) + (r_h, \nabla \cdot \mathbf{C}_h) = 0, \tag{6.4c}$$

$$(\boldsymbol{\sigma}_h, \boldsymbol{\tau}_h) - (\mathbf{u}_h \times \mathbf{B}_h, \boldsymbol{\tau}_h) = 0, \tag{6.4d}$$

$$(\mathbf{J}_h, \mathbf{M}_h) - R_m^{-1} (\mathbf{B}_h, \nabla \times \mathbf{M}_h) = 0, \tag{6.4e}$$

$$(\nabla \cdot \mathbf{B}_h, s_h) = 0. \tag{6.4f}$$

Using the fact that $\nabla \cdot \mathbf{D}_h = S_h$, we take $s_h = \nabla \cdot \mathbf{B}_h$ in (6.4f) to deduce that $\nabla \cdot \mathbf{B}_h = 0$. Furthermore, the fixed point iteration is used to solve the above nonlinear system. Since the formulation is much similar to (6.1), we omit the details.

In the numerical experiments, we choose the Mini-element to discretize the velocity and pressure, the lowest order Raviart-Thomas face element for the magnetic field and the lowest order Nédélec edge element for the current density and induced electric field. To be specific,

$$\begin{aligned} V_h &:= \{ \mathbf{v}_h \in V : \mathbf{v}_h|_K \in \mathbf{P}_{1,b}(K), \quad \forall K \in \mathcal{T}_h \}, \\ Q_h &:= \{ q_h \in H^1(\Omega) : q_h|_K \in P_1(K), \quad \forall K \in \mathcal{T}_h \} \cap Q, \\ D_h &:= \{ \mathbf{C}_h \in \mathbf{D} : \mathbf{C}_h|_K \in \mathbf{P}_0(K) + \mathbf{x}P_0(K), \quad \forall K \in \mathcal{T}_h \}, \\ W_h &:= \{ \mathbf{M}_h \in \mathbf{W} : \mathbf{M}_h|_K \in \mathbf{P}_0(K) + \mathbf{x} \times \mathbf{P}_0(K), \quad \forall K \in \mathcal{T}_h \}, \end{aligned}$$

where $P_{1,b}(K)$ is the set of linear polynomials plus a bubble, $P_{1,b}(K) = P_1(K) \oplus \{\lambda_1\lambda_2\lambda_3\lambda_4\}$, $\lambda_i, i = 1, 2, 3, 4$ is the barycentric coordinate functions on K . In particular, for the choice of the lowest order Raviart-Thomas face element for the magnetic field, we use the piecewise constant finite element space to approximate the magnetic Lagrange multiplier r ,

$$S_h = \left\{ \psi_h \in L^2_0(\Omega) : \psi_h|_K \in P_0(K), \quad \forall K \in \mathcal{T}_h \right\}.$$

Example 6.1 (Convergence rates) This example is to verify the convergence rates of finite element scheme. The computational domain is taken as $\Omega = (0, 1)^d$ and the parameters are set by $R_e = R_m = S = 1$. The right-hand sides and the boundary conditions are chosen so that the exact solutions are given by for $d = 2$,

$$\begin{aligned} \mathbf{u} &= (\cos(y), 0), \quad p = \cos(y), \quad \mathbf{B} = (0, \cos(x)), \quad J = \cos(x) \cos(y) + 1, \\ \boldsymbol{\sigma} &= \cos(x) \cos(y), \end{aligned}$$

and for $d = 3$,

$$\begin{aligned} \mathbf{u} &= (\cos(z), 0, \cos(x)), \quad p = \cos(x), \quad \mathbf{B} = (z, 0, \cos(x)), \\ \mathbf{J} &= (2x, 2y - \cos(x) \cos(z) + z \cos(x), 2z), \quad \boldsymbol{\sigma} = (0, -\cos(x) \cos(z) + z \cos(x), 0). \end{aligned}$$

It is noted that the right-hand sides are non-zero and Dirichlet boundary conditions are non-homogeneous in this test.

Table 1 Errors and convergence rates for the finite element scheme (3.11) in 2D (Example 6.1)

| h | Dofs | $\ u - u_h\ $ | $\ \nabla u - \nabla u_h\ $ | $\ p - p_h\ $ | |
|------|----------------|----------------|-----------------------------|------------------------|--------|
| 1/2 | 60 | 1.93e-02(—) | 1.16e-01(—) | 7.07e-02(—) | |
| 1/4 | 188 | 4.82e-03(2.00) | 5.73e-02(1.02) | 2.04e-02(1.80) | |
| 1/8 | 660 | 1.20e-03(2.00) | 2.85e-02(1.01) | 5.99e-03(1.77) | |
| 1/16 | 2468 | 3.00e-04(2.00) | 1.42e-02(1.00) | 1.81e-03(1.72) | |
| 1/32 | 9540 | 7.51e-05(2.00) | 7.10e-03(1.00) | 5.72e-04(1.66) | |
| h | $\ B - B_h\ $ | $\ J - J_h\ $ | $\ \sigma - \sigma_h\ $ | $\ \nabla \cdot B_h\ $ | CPU(s) |
| 1/2 | 7.46e-02(—) | 2.72e-02(—) | 2.72e-02(—) | 1.04e-15 | 0.027 |
| 1/4 | 3.76e-02(0.99) | 6.48e-03(2.07) | 6.48e-03(2.07) | 1.93e-15 | 0.057 |
| 1/8 | 1.88e-02(1.00) | 1.56e-03(2.05) | 1.56e-03(2.05) | 3.66e-15 | 0.196 |
| 1/16 | 9.42e-03(1.00) | 3.83e-04(2.03) | 3.83e-04(2.03) | 7.77e-15 | 0.774 |
| 1/32 | 4.71e-03(1.00) | 9.47e-05(2.02) | 9.47e-05(2.02) | 4.27e-14 | 3.584 |

Table 2 Errors and convergence rates for the finite element scheme (3.11) in 3D (Example 6.1)

| h | Dofs | $\ u - u_h\ $ | $\ \nabla u - \nabla u_h\ $ | $\ p - p_h\ $ | |
|------|----------------|----------------|-----------------------------|------------------------|---------|
| 1/2 | 418 | 2.75e-02(—) | 1.72e-01(—) | 9.26e-02(—) | |
| 1/4 | 2706 | 6.87e-03(2.00) | 8.55e-02(1.01) | 2.57e-02(1.85) | |
| 1/8 | 19426 | 1.72e-03(2.00) | 4.27e-02(1.00) | 7.43e-03(1.79) | |
| 1/16 | 147138 | 4.29e-04(2.00) | 2.13e-02(1.00) | 2.15e-03(1.79) | |
| h | $\ B - B_h\ $ | $\ J - J_h\ $ | $\ \sigma - \sigma_h\ $ | $\ \nabla \cdot B_h\ $ | CPU(s) |
| 1/2 | 1.31e-01(—) | 6.32e-01(—) | 1.88e-01(—) | 3.12e-15 | 0.513 |
| 1/4 | 6.54e-02(1.00) | 3.17e-01(1.00) | 9.50e-02(0.99) | 4.33e-15 | 5.911 |
| 1/8 | 3.27e-02(1.00) | 1.58e-01(1.00) | 4.76e-02(1.00) | 7.24e-15 | 60.081 |
| 1/16 | 1.63e-02(1.00) | 7.92e-02(1.00) | 2.38e-02(1.00) | 1.52e-14 | 407.982 |

We display the degrees of freedom (Dofs), computational time (CPU), the errors and the convergence orders of the proposed scheme in Table 1 for $d = 2$ and Table 2 for $d = 3$. From these tables, we observe that the errors of all variables become smaller and smaller as the mesh is refined, and the expected orders for all variables are obtained. This verifies our theoretical analysis in Theorem 5.1. Note that since we approximate the current density J and induced magnetic field σ by using the linear Lagrange finite element in 2D and the lowest-order Nédélec edge element in 3D, the convergence rate of the L^2 -norm is second-order in 2D and becomes first-order in 3D. Specifically, the approximate solutions yield $\|\nabla \cdot B_h\|$ in the order of $10^{-15} \sim 10^{-14}$, which is almost divergence-free. However, the discrete magnetic field is exactly divergence-free according to Theorem 4.1. We think this is mainly due to the numerical integral errors and rounding errors.

For comparison, we repeat the numerical tests by using the finite element scheme (6.4) with $r = 0$ and list the results in Tables 3–4. As we can see, the results are

Table 3 Errors and convergence rates for the finite element scheme (6.4) in 2D (Example 6.1)

| h | Dofs | $\ u - u_h\ $ | $\ \nabla u - \nabla u_h\ $ | $\ p - p_h\ $ | $\ r - r_h\ $ |
|------|----------------|----------------|-----------------------------|------------------------|---------------|
| 1/2 | 68 | 1.93e-02(—) | 1.16e-01(—) | 7.07e-02(—) | 3.75401e-16 |
| 1/4 | 220 | 4.82e-03(2.00) | 5.73e-02(1.02) | 2.04e-02(1.80) | 1.62706e-15 |
| 1/8 | 788 | 1.20e-03(2.00) | 2.85e-02(1.01) | 5.99e-03(1.77) | 2.42608e-15 |
| 1/16 | 2980 | 3.00e-04(2.00) | 1.42e-02(1.00) | 1.81e-03(1.72) | 1.49863e-15 |
| 1/32 | 11588 | 7.51e-05(2.00) | 7.10e-03(1.00) | 5.72e-04(1.66) | 2.77329e-15 |
| h | $\ B - B_h\ $ | $\ J - J_h\ $ | $\ \sigma - \sigma_h\ $ | $\ \nabla \cdot B_h\ $ | CPU(s) |
| 1/2 | 7.46e-02(—) | 2.72e-02(—) | 2.72e-02(—) | 5.66e-16 | 0.019 |
| 1/4 | 3.76e-02(0.99) | 6.48e-03(2.07) | 6.48e-03(2.07) | 6.94e-15 | 0.054 |
| 1/8 | 1.88e-02(1.00) | 1.56e-03(2.05) | 1.56e-03(2.05) | 3.71e-14 | 0.225 |
| 1/16 | 9.42e-03(1.00) | 3.83e-04(2.03) | 3.83e-04(2.03) | 3.35e-14 | 0.888 |
| 1/32 | 4.71e-03(1.00) | 9.47e-05(2.02) | 9.47e-05(2.02) | 7.02e-14 | 3.992 |

Table 4 Errors and convergence rates for the finite element scheme (6.4) in 3D (Example 6.1)

| h | Dofs | $\ u - u_h\ $ | $\ \nabla u - \nabla u_h\ $ | $\ p - p_h\ $ | $\ r - r_h\ $ |
|------|----------------|----------------|-----------------------------|------------------------|---------------|
| 1/2 | 418 | 2.75e-02(—) | 1.72e-01(—) | 9.26e-02(—) | 7.73e-15 |
| 1/4 | 2706 | 6.87e-03(2.00) | 8.55e-02(1.01) | 2.57e-02(1.85) | 2.45e-14 |
| 1/8 | 19426 | 1.72e-03(2.00) | 4.27e-02(1.00) | 7.43e-03(1.79) | 1.38e-13 |
| 1/16 | 147138 | 4.29e-04(2.00) | 2.13e-02(1.00) | 2.15e-03(1.79) | 2.67e-13 |
| h | $\ B - B_h\ $ | $\ J - J_h\ $ | $\ \sigma - \sigma_h\ $ | $\ \nabla \cdot B_h\ $ | CPU(s) |
| 1/2 | 1.31e-01(—) | 6.32e-01(—) | 1.88e-01(—) | 2.83e-13 | 0.682 |
| 1/4 | 6.54e-02(1.00) | 3.17e-01(1.00) | 9.50e-02(0.99) | 4.00e-12 | 6.437 |
| 1/8 | 3.27e-02(1.00) | 1.58e-01(1.00) | 4.76e-02(1.00) | 8.73e-12 | 65.432 |
| 1/16 | 1.63e-02(1.00) | 7.92e-02(1.00) | 2.38e-02(1.00) | 7.46e-12 | 440.747 |

almost the same as the previous ones, but the finite element scheme (6.4) requires more degrees of freedom and thus cost much computational time than our scheme in most cases. Thus, our scheme has a little upper hand in saving the computational time.

Example 6.2 (Hartmann flow) This example is to verify the convergence rate of the Hartmann flow. This problem is the MHD version of the classical Poiseuille flow, which describes the flow of a conducting fluid through a channel in the presence of a transverse magnetic field. Herein, we consider the channel $\Omega = (-1/2, 1/2)^2$ and the transverse field $B_d = (1, 0)$. With appropriate boundary conditions and $f = \mathbf{0}$, this problem has the explicit analytic solution [1, 8, 16, 20, 25],

$$u = (u_1(y), 0), \quad B = (B_1(y), 1), \quad p = -Gx - \frac{S}{2} B_1^2(y),$$

where

$$\begin{aligned}
 H_a &= \sqrt{SR_e}, \quad G = \frac{2H_a \sinh(H_a/2)}{R_e(\cosh(H_a/2) - 1)}, \\
 u_1(y) &= \frac{GRe}{2H_a \tanh(H_a/2)} \left(1 - \frac{\cosh(yH_a)}{\cosh(H_a/2)} \right), \\
 B_1(y) &= \frac{G}{2S} \left(\frac{\sinh(yH_a)}{\sinh(H_a/2)} - 2y \right).
 \end{aligned}$$

The analytical solutions for the current density and induced electric field are computed by using (2.3d) and (2.3c). In the test, we impose inhomogeneous Dirichlet boundary conditions from the exact solution. Note that the parameter $H_a = \sqrt{SR_e} = LB_0\sqrt{\sigma/\eta}$ is the well-known Hartmann number, and there are some typos about this physical parameter in [16]. The physical parameters are taken as $R_e = R_m = S = 1$.

The numerical results for our scheme are given in Table 5. We find that the predicted convergence rates are achieved asymptotically for all variables. In addition, the current density \mathbf{J} and induced magnetic field σ are of second-order accuracy again due to the usage of using the linear Lagrange finite element. The quantity $\|\nabla \cdot \mathbf{B}_h\|$ is observed in the order of $10^{-16} \sim 10^{-14}$, which verifies the structure-preserving property of our scheme.

Similar to the previous example, we rerun the numerical test by using the finite element scheme (6.4) with $r = 0$ and display the results in Table 6. As we can see, the results are almost the same as the previous ones, but the finite element scheme (6.4) requires more degrees of freedom and thus cost much computational time than our scheme in most cases. Thus, our scheme has a little upper hand in saving the computational time.

In Fig. 1, we plot the velocity, the magnetic field and the current density of numerical solutions with the mesh size $h = 1/100$. To characterize the numerical solution in a quantitative way, we further display the corresponding errors in Fig. 2. It is obvious that the numerical solution is quite close to the analytical solution. Based on the results, we can conclude that our scheme is good enough to simulate the Hartmann flow problem.

Example 6.3 (Driven Cavity Flow) In this example, we consider a well-known benchmark problem in fluid dynamics, known as driven cavity flow. It is a model of the flow in a cavity with the lid moving in one direction under the external magnetic field. When the external magnetic field is zero, the problem becomes the classical hydrodynamic lid-driven cavity problem. For this end, we set the computational domain by $\Omega = (0, 1)^d$ and the right-hand side by $\mathbf{f} = \mathbf{0}$. The remaining setting will be specified later.

We first consider the two-dimensional lid-driven cavity problem, namely, $d = 2$, see Fig. 3. The mesh size is set by $h = 1/100$ and the coupling number is chosen as $S = 1$. Let $\mathbf{B}_b = (1, 0)$, $\mathbf{u}_b = (v, 0)$ where $v \in C^1(\bar{\Omega})$ and satisfies

$$v(x, 1) = 1 \quad \text{and} \quad v(x, y) = 0 \quad \forall y \in [0, 1 - h],$$

Table 5 Errors and convergence rates for the finite element scheme (3.11) in 2D (Example 6.2)

| h | Dofs | $\ u - u_h\ $ | $\ \nabla u - \nabla u_h\ $ | $\ p - p_h\ $ |
|------|------|----------------|-----------------------------|----------------|
| 1/2 | 60 | 5.66e-02(—) | 3.40e-01(—) | 2.07e-01(—) |
| 1/4 | 188 | 1.42e-02(2.00) | 1.68e-01(1.01) | 6.10e-02(1.76) |
| 1/8 | 660 | 3.54e-03(2.00) | 8.38e-02(1.01) | 1.82e-02(1.74) |
| 1/16 | 2468 | 8.83e-04(2.00) | 4.18e-02(1.00) | 5.51e-03(1.72) |
| 1/32 | 9540 | 2.21e-04(2.00) | 2.09e-02(1.00) | 1.73e-03(1.67) |

| h | $\ B - B_h\ $ | $\ J - J_h\ $ | $\ \sigma - \sigma_h\ $ | $\ \nabla \cdot B_h\ $ | CPU(s) |
|------|----------------|----------------|-------------------------|------------------------|--------|
| 1/2 | 1.07e-02(—) | 5.92e-02(—) | 5.92e-02(—) | 7.85e-16 | 0.020 |
| 1/4 | 6.34e-03(0.76) | 1.47e-02(2.01) | 1.47e-02(2.01) | 1.75e-15 | 0.036 |
| 1/8 | 3.27e-03(0.96) | 3.63e-03(2.01) | 3.63e-03(2.01) | 4.33e-15 | 0.142 |
| 1/16 | 1.64e-03(0.99) | 9.03e-04(2.01) | 9.03e-04(2.01) | 9.76e-15 | 0.508 |
| 1/32 | 8.23e-04(1.00) | 2.25e-04(2.01) | 2.25e-04(2.01) | 3.07e-14 | 2.449 |

Table 6 Errors and convergence rates for the finite element scheme (6.4) in 2D (Example 6.2)

| h | Dofs | $\ u - u_h\ $ | $\ \nabla u - \nabla u_h\ $ | $\ p - p_h\ $ | $\ r - r_h\ $ |
|------|-------|----------------|-----------------------------|----------------|---------------|
| 1/2 | 68 | 5.66e-02(—) | 3.40e-01(—) | 2.07e-01(—) | 4.68e-17 |
| 1/4 | 220 | 1.42e-02(2.00) | 1.68e-01(1.01) | 6.10e-02(1.76) | 1.81e-15 |
| 1/8 | 788 | 3.54e-03(2.00) | 8.38e-02(1.01) | 1.82e-02(1.74) | 2.91e-14 |
| 1/16 | 2980 | 8.83e-04(2.00) | 4.18e-02(1.00) | 5.51e-03(1.72) | 1.36e-13 |
| 1/32 | 11588 | 2.21e-04(2.00) | 2.09e-02(1.00) | 1.73e-03(1.67) | 2.11e-13 |

| h | $\ B - B_h\ $ | $\ J - J_h\ $ | $\ \sigma - \sigma_h\ $ | $\ \nabla \cdot B_h\ $ | CPU(s) |
|------|----------------|----------------|-------------------------|------------------------|--------|
| 1/2 | 1.07e-02(—) | 5.92e-02(—) | 5.92e-02(—) | 8.46e-16 | 0.021 |
| 1/4 | 6.34e-03(0.76) | 1.47e-02(2.01) | 1.47e-02(2.01) | 8.38e-15 | 0.039 |
| 1/8 | 3.27e-03(0.96) | 3.63e-03(2.01) | 3.63e-03(2.01) | 4.24e-13 | 0.154 |
| 1/16 | 1.64e-03(0.99) | 9.03e-04(2.01) | 9.03e-04(2.01) | 1.51e-13 | 0.604 |
| 1/32 | 8.23e-04(1.00) | 2.25e-04(2.01) | 2.25e-04(2.01) | 1.12e-13 | 2.832 |

the boundary conditions are set by

$$u = u_b, \quad B \cdot n = B_b \cdot n, \quad J \times n = \mathbf{0}, \quad \sigma \times n = \mathbf{0} \quad \text{on } \Gamma.$$

We perform numerical tests of fixed magnetic Reynolds number $R_m = 1$ and different Reynolds numbers $R_e = 1, 500, 5000$. Figure 4 plots the streamlines of the velocity. We can see that as the Reynolds number increases, the large primary vortex moves upwards due to the increased Lorentz force and the new eddies with a certain aspect ratio emerge on the lower cavity wall and they may also detach from the lower wall depending on their aspect ratio. Finally, the multiple high-aspect-ratio cellular structures form within the cavity. Therefore, we conclude that as the Reynolds number increases, the fluid yields more thin eddies and tends to be stratified.

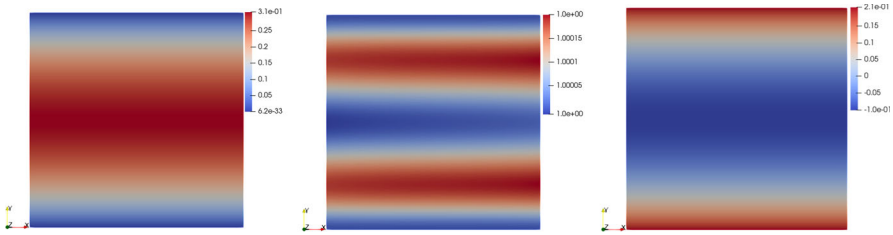


Fig. 1 Numerical results of $|u_h|$, $|B_h|$ and J_h with $h = 1/100$. (Example 6.2)

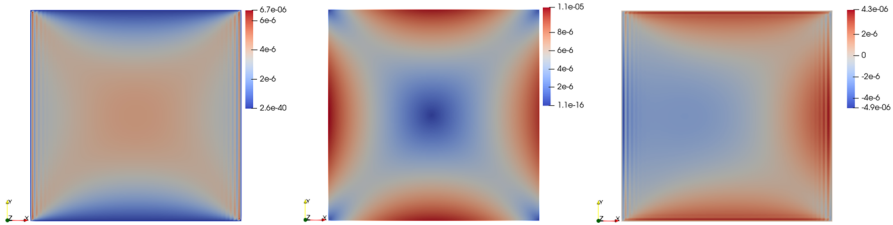
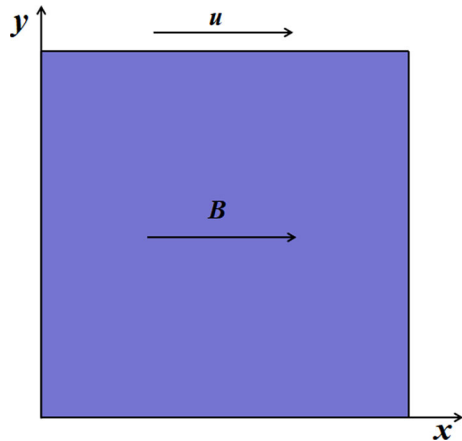


Fig. 2 Numerical results of $|u - u_h|$, $|B - B_h|$ and $J - J_h$ with $h = 1/100$. (Example 6.2)

Fig. 3 Geometry of lid driven cavity in 2D



To study further the braking effect of the magnetic field, we rerun with the fixed Reynolds number $R_e = 1000$, Reynolds number $R_m = 1$ and different coupling numbers $S = 1, 2, 4, 8, 16, 32$. The corresponding streamlines of the velocity are plotted in Fig. 5. From the obtained results, we can see that the coupling number has a great influence on the flow structure. Similar to the previous tests, the number of cells increases with the increase in the coupling number. Hence, the expectant braking effect of the magnetic field on the flow is demonstrated. The obtained results qualitatively coincide with the results discussed in [2, 24, 29].

Next, we turn to study the braking effect of the magnetic field for the three-dimensional lid-driven cavity problem, namely, $d = 3$, see Fig. 6. Similar to the two-dimensional case, let $B_b = (1, 0, 0)$, $u_b = (v, 0, 0)$ where $v \in C^1(\bar{\Omega})$ and

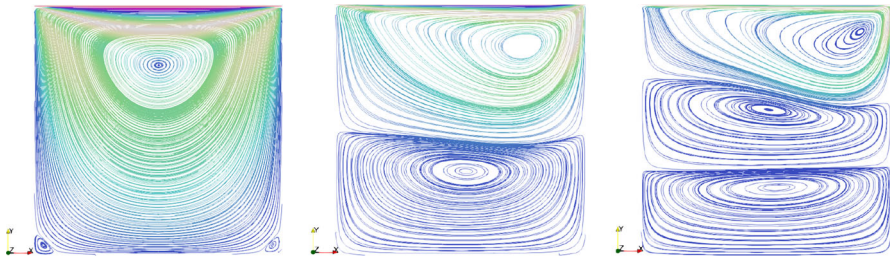


Fig. 4 Streamlines for the velocity with $Re = 1, 500, 5000$ for the lid-driven cavity problem in 2D

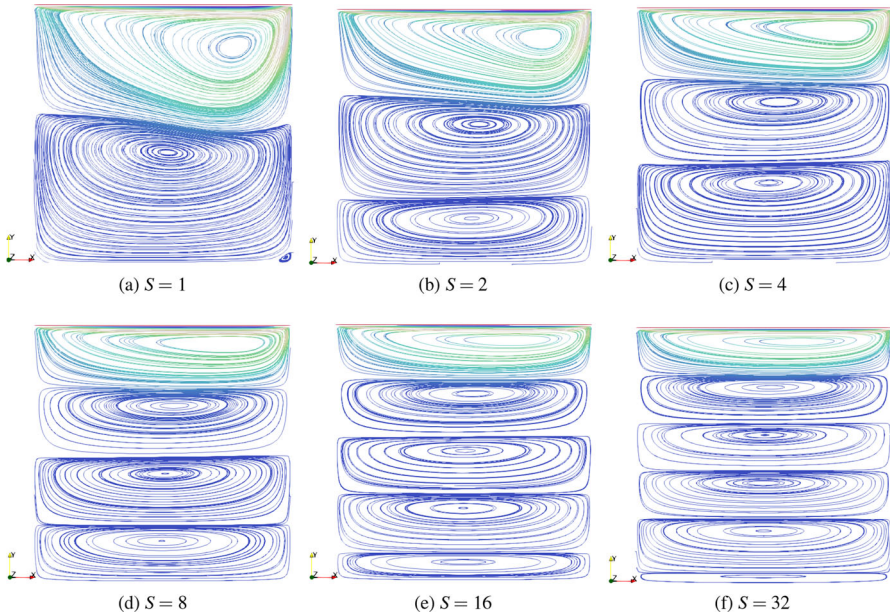


Fig. 5 Streamlines for the velocity with $Re = 1000, R_m = 1$ and different coupling numbers for the lid-driven cavity problem in 2D

satisfies

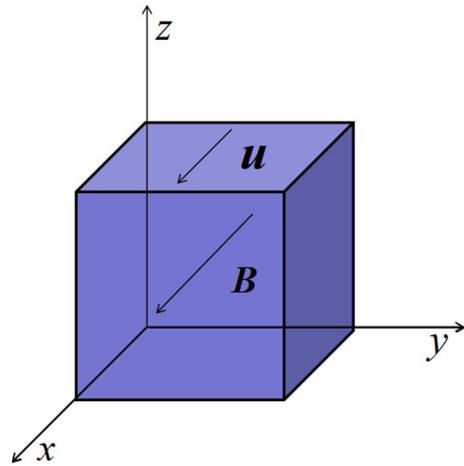
$$v(x, y, 1) = 1 \quad \text{and} \quad v(x, y, z) = 0 \quad \forall z \in [0, 1 - h],$$

the boundary conditions are set by

$$\mathbf{u} = \mathbf{u}_b, \quad \mathbf{B} \cdot \mathbf{n} = \mathbf{B}_b \cdot \mathbf{n}, \quad \mathbf{J} \times \mathbf{n} = \mathbf{0}, \quad \boldsymbol{\sigma} \times \mathbf{n} = \mathbf{0} \quad \text{on } \Gamma.$$

In the computation, we set the mesh size by $h = 1/32$, fix the Reynolds number as $Re = 100$ and the magnetic Reynolds number as $R_m = 1$, and vary the coupling number gradually. In Fig. 7, we show the streamlines of velocity on the cross-section $y = 0.5$. From these figures, we can see again that as the coupling number increases, the fluid yields more thin eddies and tends to be stratified. Thus, the effects of the

Fig. 6 Geometry of lid driven cavity in 3D



coupling number on the flow structure for the three-dimensional problem are similar to the two-dimensional problem in our model. To deliver more details of the discrete solutions, we plot the isosurfaces for the magnetic field, current density and induced magnetic field with $S = 40$ in Fig. 8. From these figures, we can see how the fluid influences the electromagnetic fields.

7 Concluding remarks

In this paper, we propose and analyze a new structure-preserving finite element scheme for the stationary MHD system with magnetic-current formulation on general Lipschitz domains. In mixed finite element approximation, we discretize the hydrodynamic unknowns by inf-sup stable velocity-pressure finite element pairs and discretize the current density, the induced electric field and the magnetic field by using the edge-edge-face elements from a discrete de-Rham complex pair. Thanks to discrete differential forms and finite element exterior calculus, the proposed scheme preserves the divergence-free property exactly for the magnetic induction on the discrete level. Furthermore, we rigorously establish the well-posedness of the discrete problem and prove the error estimates of the finite element scheme under weak regularity assumptions. Numerical results illustrate the theoretical results and demonstrate the efficiency of the proposed method. In the future, we will consider efficient iterative methods and fast solvers for the MHD equations.

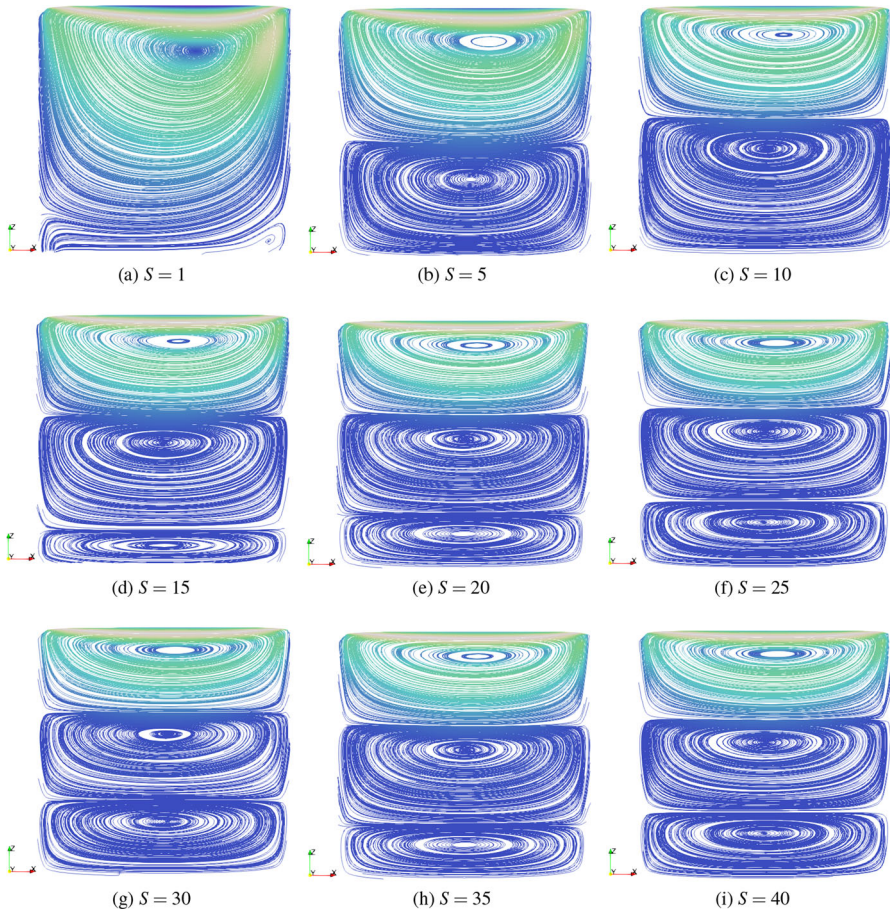


Fig. 7 Streamlines for the velocity with $R_e = 100$, $R_m = 1$ and different coupling numbers for the lid-driven cavity problem in 3D

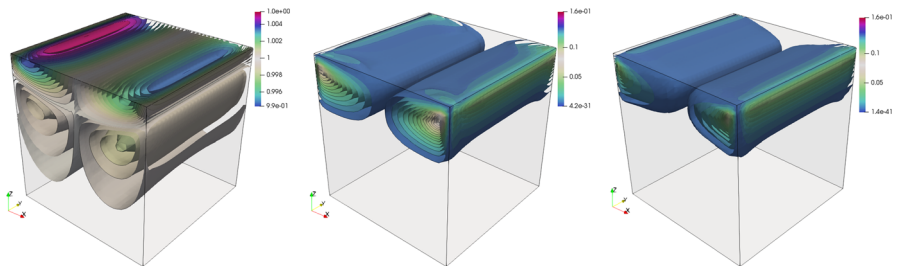


Fig. 8 Isosurfaces for the magnetic field, current density and induced electric field with $S = 40$ for the lid-driven cavity problem in 3D

Acknowledgements The authors wish to thank the anonymous referees and the associate editor for many constructive comments that improved the paper.

Author Contributions XZ: conceptualization, methodology, formal analysis, writing, review. SD: visualization, validation, review. All authors reviewed the manuscript.

Funding The first author's research is supported in part by the National Natural Science Foundation of China under Grant 12201575 and China Postdoctoral Science Foundation under Grant 2022M722878. The second author's research is supported in part by Xinjiang Graduate Student Research Innovation Project under Grant XJ2023G081.

Availability of data and materials Data sharing is not applicable to this article as no datasets were generated or analyzed during the current study.

Declarations

Conflict of interest The authors declare no competing interests.

Ethical approval Not applicable.

References

1. Adler, J.H., Benson, T.R., Cyr, E.C., Farrell, P.E., MacLachlan, S.P., Tuminaro, R.S.: Monolithic multigrid methods for magnetohydrodynamics. *SIAM J. Sci. Comput.* **43**(5), S70–S91 (2021)
2. Ata, K., Sahin, M.: A facebased monolithic approach for the incompressible magnetohydrodynamics equations. *Int. J. Numer. Methods Fluids* **92**(5), 347–371 (2020)
3. Boffi, D., Brezzi, F., Fortin, M.: Mixed finite element methods and applications. Springer Series in Computational Mathematics, vol. 44. Springer, Heidelberg (2013)
4. Brackbill, J.U., Barnes, D.C.: The effect of nonzero $\nabla \cdot \mathbf{B}$ on the numerical solution of the magnetohydrodynamic equations. *J. Comput. Phys.* **35**(3), 426–430 (1980)
5. Dai, W., Woodward, P.R.: On the divergence-free condition and conservation laws in numerical simulations for supersonic magnetohydrodynamic flows. *Astrophys. J.* **494**(1), 317 (1998)
6. Davidson, P.A.: An introduction to magnetohydrodynamics. Cambridge Texts in Applied Mathematics, Cambridge University Press, Cambridge (2001)
7. Gao, H., Qiu, W.: A semi-implicit energy conserving finite element method for the dynamical incompressible magnetohydrodynamics equations. *Comput. Methods Appl. Mech. Eng.* **346**, 982–1001 (2019)
8. Gerbeau, J.F., Le Bris, C., Lelièvre, T.: Mathematical methods for the magnetohydrodynamics of liquid metals. Numerical Mathematics and Scientific Computation, Oxford University Press, Oxford (2006)
9. Girault, V., Raviart, P.A.: Finite element methods for Navier-Stokes equations, Springer Series in Computational Mathematics, vol. 5. Springer-Verlag, Berlin (1986). Theory and algorithms
10. Goedbloed, J.P., Keppens, R., Poedts, S.: Advanced Magnetohydrodynamics: With Applications to Laboratory and Astrophysical Plasmas. Cambridge University Press, Cambridge (2010)
11. Goedbloed, J.P.H., Poedts, S.: Principles of Magnetohydrodynamics: With Applications to Laboratory and Astrophysical Plasmas. Cambridge University Press, Cambridge (2004)
12. Gunzburger, M.D., Meir, A.J., Peterson, J.S.: On the existence, uniqueness, and finite element approximation of solutions of the equations of stationary, incompressible magnetohydrodynamics. *Math. Comput.* **56**(194), 523–563 (1991)
13. He, Y.: Unconditional convergence of the Euler semi-implicit scheme for the three-dimensional incompressible MHD equations. *IMA J. Numer. Anal.* **35**(2), 767–801 (2015)
14. Hecht, F.: New development in FreeFem++. *J. Numer. Math.* **20**(3–4), 251–265 (2012)
15. Hiptmair, R., Li, L., Mao, S., Zheng, W.: A fully divergence-free finite element method for magnetohydrodynamic equations. *Math. Models Methods Appl. Sci.* **28**(4), 659–695 (2018)
16. Hu, K., Ma, Y., Xu, J.: Stable finite element methods preserving $\nabla \cdot \mathbf{B} = 0$ exactly for MHD models. *Numer. Math.* **135**(2), 371–396 (2017)

17. Hu, K., Xu, J.: Stable magnetic field-current finite element formulation for magnetohydrodynamics system (in Chinese). *Sci. Sin. Math.* **46**(7), 967–980 (2016)
18. Hu, K., Xu, J.: Structure-preserving finite element methods for stationary MHD models. *Math. Comput.* **88**(316), 553–581 (2019)
19. John, V.: Finite element methods for incompressible flow problems. Springer Series in Computational Mathematics, vol. 51. Springer, Cham (2016)
20. Laakmann, F., Farrell, P.E., Mitchell, L.: An augmented Lagrangian preconditioner for the magnetohydrodynamics equations at high Reynolds and coupling numbers. *SIAM J. Sci. Comput.* **44**(4), B1018–B1044 (2022)
21. Li, L., Zhang, D., Zheng, W.: A constrained transport divergence-free finite element method for incompressible MHD equations. *J. Comput. Phys.* **428**(109980), 22 (2021)
22. Li, X., Li, L.: A conservative finite element solver for the induction equation of resistive MHD: vector potential method and constraint preconditioning. *J. Comput. Phys.* **466**(111416), 20 (2022)
23. Ma, Y., Xu, J., Zhang, G.D.: Error estimates for structure-preserving discretization of the incompressible MHD system. [arXiv: arXiv:1608.03034](https://arxiv.org/abs/1608.03034) (2016)
24. Marioni, L., Bay, F., Hachem, E.: Numerical stability analysis and flow simulation of lid-driven cavity subjected to high magnetic field. *Phys. Fluids* **28**, 057102 (2016)
25. Phillips, E.G., Elman, H.C., Cyr, E.C., Shadid, J.N., Pawlowski, R.P.: A block preconditioner for an exact penalty formulation for stationary MHD. *SIAM J. Sci. Comput.* **36**(6), B930–B951 (2014)
26. Prohl, A.: Convergent finite element discretizations of the nonstationary incompressible magnetohydrodynamics system. *M2AN Math. Model. Numer. Anal.* **42**(6), 1065–1087 (2008)
27. Qiu, W., Shi, K.: Analysis of a semi-implicit structure-preserving finite element method for the nonstationary incompressible magnetohydrodynamics equations. *Comput. Math. Appl.* **80**(10), 2150–2161 (2020)
28. Schötzau, D.: Mixed finite element methods for stationary incompressible magneto-hydrodynamics. *Numer. Math.* **96**(4), 771–800 (2004)
29. Su, H., Feng, X., Huang, P.: Iterative methods in penalty finite element discretization for the steady MHD equations. *Comput. Methods Appl. Mech. Eng.* **304**, 521–545 (2016)
30. Tóth, G.: The $\nabla \cdot \mathbf{B} = 0$ constraint in shock-capturing magnetohydrodynamics codes. *J. Comput. Phys.* **161**(2), 605–652 (2000)
31. Yang, J., Mao, S.: Second order fully decoupled and unconditionally energy-stable finite element algorithm for the incompressible MHD equations. *Appl. Math. Lett.* **121**(107467), 8 (2021)
32. Zhang, G., He, Y., Yang, D.: Analysis of coupling iterations based on the finite element method for stationary magnetohydrodynamics on a general domain. *Comput. Math. Appl.* **68**(7), 770–788 (2014)
33. Zhang, G., Yang, J., Bi, C.: Second order unconditionally convergent and energy stable linearized scheme for MHD equations. *Adv. Comput. Math.* **44**(2), 505–540 (2018)
34. Zhang, X., Ding, Q.: Coupled iterative analysis for stationary inductionless magnetohydrodynamic system based on charge-conservative finite element method. *J. Sci. Comput.* **88**(2), 32 (2021)

Publisher's Note Springer Nature remains neutral with regard to jurisdictional claims in published maps and institutional affiliations.

Springer Nature or its licensor (e.g. a society or other partner) holds exclusive rights to this article under a publishing agreement with the author(s) or other rightsholder(s); author self-archiving of the accepted manuscript version of this article is solely governed by the terms of such publishing agreement and applicable law.